AMERICAN MUSEUM NOVITATES

Number 3897, 41 pp. March 21, 2018

A New Species of *Forstercooperia* (Perissodactyla: Paraceratheriidae) from Northern China with a Systematic Revision of Forstercooperiines

HAI-BING WANG,[1, 2, 3] BIN BAI,[1, 2, 4] JIN MENG,[4, 1] YUAN-QING WANG[1, 2, 3]

ABSTRACT

Forstercooperiines are a group of large, primitive rhinocerotoids that are commonly regarded as ancestral to later giant rhinos. However, the type genus of forstercooperiines, the Middle Eocene *Forstercooperia*, is one of the most poorly known rhinocerotoids, and is represented only by fragmentary material. Here we name a new species, *Forstercooperia ulanshirehensis*, based on five specimens, including a well-preserved cranium and a pair of complete mandibles. This new material was collected from the Ulan Shireh Formation in the western part of the Erlian Basin and the Irdin Manha Formation in the eastern part of the Erlian Basin, northern China. These specimens provide the most complete craniodental remains of *Forstercooperia* sensu stricto (excluding *Pappaceras*), and on this basis the species-level taxonomy of forstercooperiines is thoroughly revised and six species of two genera are considered as valid. Specimens previously assigned to "*Forstercooperia minuta*" are reassigned to different species based on the revised diagnoses. All equivocal specimens that were thought to have an affinity with Forstercooperiinae are briefly discussed. Based on a new character matrix, phylogenetic analyses fully resolve the relationships of early rhinocerotoids, including the recovery of *Forstercooperia* and *Pappaceras* as sister groups. The occurrence of *Forstercooperia ulanshirehensis* in the eastern and western Erlian Basin is indicative of age correlation between the lower part of the Ulan Shireh Formation and the Irdin Manha Formation.

[1] Key Laboratory of Vertebrate Evolution and Human Origins of Chinese Academy of Sciences, Institute of Vertebrate Paleontology and Paleoanthropology, Chinese Academy of Sciences, Beijing.
[2] CAS Center for Excellence in Life and Paleoenvironment, Beijing.
[3] College of Earth and Planetary Sciences, University of Chinese Academy of Sciences, Beijing.
[4] Division of Paleontology, American Museum of Natural History, New York.

 ISSN 0003-0082

INTRODUCTION

Forstercooperines are a group of primitive rhinocerotoids from the Asian Eocene that have a close affinity to paraceratheres (giant rhinos) (Lucas and Sobus, 1989; Qiu and Wang, 2007). Although this group has been studied since 1938 (Wood, 1938), the fossil record of forstercooperiines is not so abundant as that of other rhinocerotoid groups. There have been a few revisions of the systematics of this group (Radinsky, 1967; Lucas et al., 1981; Lucas and Sobus, 1989), in which forstercooperiines were considered as monogeneric by these authors. For example, *Pappaceras* Wood, 1963, was synonymized with *Forstercooperia* Wood, 1939. However, evidence showing distinct features between *Pappaceras* and *Forstercooperia* has cast doubt on this consideration (Qiu and Wang, 2007; Bai and Wang, 2012; Wang et al., 2016). In particular, on the basis of a recently reported, well-preserved specimen of *Pappaceras*, the phylogenetic relationships of early rhinoceorotoids has been extensively explored and discussed, in which *Pappaceras* was shown not readily synonymous with *Forstercooperia* (Wang et al., 2016). Nonetheless, the phylogenetic relationships within forstercooperiines still remain open to discussion of the paraphyly of *Pappaceras*, primarily because of character conflicts and numerous missing character states for several taxa in the data matrix, particularly *Forstercooperia*, which is one of the most poorly known rhinocerotoids, represented by only a few fragmentary specimens (Wood, 1938; Chow et al., 1974; Qiu and Wang, 2007). The morphology of *Forstercooperia* is significant for further exploration of the phylogenetic relationships of early rhinocerotoids as well as forstercooperiines.

Since *Forstercooperia* was established in 1938, four genera have been included in forstercooperiines, including *Cooperia* Wood, 1938; *Imequincisoria* Wang, 1976; *Forstercooperia* Wood, 1939; and *Pappaceras* Wood, 1963. *Cooperia* was originally erected based on the type specimen AMNH 20116, which was already occupied by a nematode genus, so it was replaced by *Forstercooperia* (Wood, 1938). The two species of *Imequincisoria* have been assigned to *Forstercooperia* and *Juxia* respectively, as proposed by Qiu and Wang (2007), and thus the generic name *Imequincisoria* should be abandoned. Wood (1963) established *Pappaceras* as a well-documented Eocene rhinocerotoid ancestral to later rhinocerotids. In contrast, Radinsky (1967) and Lucas et al. (1981) suggested that *Pappaceras* was a junior synonym of *Forstercooperia* in the context of assigning forstercooperiines to Hyracodontidae. They assigned both Asian and North American materials to this subfamily (Radinsky, 1967; Lucas et al., 1981). Subsequently, this bulk assignment to forstercooperiines was challenged by the erection of the genus *Uintaceras* to encompass most of the North American materials formerly assigned to forstercooperiines (Holbrook and Lucas, 1997), restricting the distribution and evolution of forstercooperiines to Asia. Furthermore, new stratigraphical and morphological evidence lend more support to separating *Pappaceras* from *Forstercooperia* (Meng et al., 2007; Qiu and Wang, 2007; Wang et al., 2010, 2016). Recent field investigation clarifies that the specimens of *Forstercooperia* are mainly from the Irdin Manha Formation or equivalent deposits, whereas all specimens of *Pappaceras* to date have been unearthed in the Arshanto Formation or equivalent sediments. Moreover, there is still a distinct morphological gap between *Forstercooperia* and *Pappaceras*, as recently suggested (Qiu and Wang, 2007; Bai and Wang, 2012; Wang et al., 2016) and that will be discussed in detail in this study.

Among forstercooperiines, *Pappaceras* is the earliest representative, appearing first in the late early Eocene (Wang et al., 2016). It has a fairly abundant fossil record, represented by three species known from fragmentary craniodental elements (Wood, 1963; Lucas et al., 1981; Wang et al., 2016). In contrast, the type genus *Forstercooperia*, which is Irdinmanhan in Asian Land Mammal Ages, has a poor fossil record and consists of *F. totadentata* (the type species) and *F. mazhuangensis* that are represented only by a cranial fragment and a few dental fragments, respectively (Wood, 1938; Wang, 1976; Qiu and Wang, 2007). In the present study, we erect a new species of *Forstercooperia*, based on five specimens unearthed from the Eocene sediments in Erlian Basin, Nei Mongol, China, including a well-preserved cranium and a pair of complete mandibles. The new finding is fundamental for the comparative study of tapiromorphs, filling the large gap of the craniodental morphology of *Forstercooperia* and narrowing the morphological gap between forstercooperiines and paraceratheriines. Additionally, it has great potential to further resolve the phylogenetic relationships of forstercooperiines.

MATERIALS AND METHODS

Three new specimens (IVPP V20154, V20155, V20156) were recovered from the Irdin Manha Formation in the Irdin Manha site in the expeditions of the Institute of Vertebrate Paleontology and Paleoanthropology over the last 15 years (fig. 1). This is the type locality for the holotype of *F. totadentata* (AMNH 20116) (Wood, 1938). The other two specimens (AMNH 21608, 22101) were collected from the Ulan Shireh Formation at the Wulantaolegai site (previously known as "4 miles north of Tukhum") and the Wulanhuxiu site (previously known as "8 miles north of Tukhum Lamasery"), respectively, by the Central Asian Expeditions of the American Museum of Natural History in the 1920s (fig. 1) (Wang et al., 2012). The five specimens are not directly associated with each other, the new specimens were recovered in equivalent sediments in East and West parts of Erlian Basin as suggested in recent studies that the upper part of the Ulan Shireh Formation likely correlative to Irdinmanhan sediments (Wang et al., 2012). Anatomical terminology follows Qiu and Wang (2007), in which the entolophid corresponds to the "hypolophid" of Bai et al. (2010) and Mihlbachler (2008), and the hypolophid corresponds to the "cristid obliqua." A list of specimens examined for this study is provided in the appendix (see also table 1). Measurements were taken using digital calipers and are given in millimeters.

For phylogenetic analyses, we adopted the character list from Wang et al. (2016) and coded the character states of the new species based on the new specimens reported in the present study. Following that character list, two polymorphic characters (chars. 29 and 30) are set as additive (or ordered) in this study. The phylogenetic analyses were performed using TNT 1.1 with the New Technology search method (Goloboff et al., 2008), under equally weighted parsimony. As conventionally used for large data sets, 200 ratchet iterations (Nixon, 1999), 100 drift cycles, and 10 rounds of tree fusion (Goloboff, 1999) were applied to conduct comprehensive searches in the phylogenetic analyses. The data matrix has been archived in Morphobank (http://morphobank.org/permalink/?P2535).

Institutional abbreviations: AMNH, American Museum of Natural History; CMNH, Carnegie Museum of Natural History; IVPP, Institute of Vertebrate Paleontology and Paleoanthropology; PGM, Geological Museum of China (Peking Geological Museum); UCMP, University of California Museum of Paleontology.

SYSTEMATICS

Mammalia Linnaeus, 1758

Perissodactyla Owen, 1848

Rhinocerotoidea Gray, 1825

Paraceratheriidae Osborn, 1923

Forstercooperiinae Kretzoi, 1940

Type genus: *Forstercooperia* Wood, 1938.

Included genus: The type genus and *Pappaceras* Wood, 1963.

Revised diagnosis: Small paraceratheriid of medium to large body size. Skull length about 390–455 mm and length of upper/lower molar series about 70–130 mm. Skull dolichocephalic. Premaxilla in contact with nasal; preorbital fossa shallow; maxilla high; facial exposure of lacrimal large; frontal wide between orbits and followed by a distinct flange overhanging postorbital cavity; postglenoid foramen absent. Upper premolars primitive with weak metalophs, P3–4 transversely wide; ribs of upper premolars distinct. Antecrochet of M1 usually present; metastyle of M2 elongated. Lower premolars primitive with weak entoconid of p4 present in some species; protolophid of lower molars anterolingually extended. Loss of P1/p1 present in some species. Cingulum/cingulid of cheek teeth usually present at anterior, lingual, and posterior bases. Differs from other rhinocerotoids in having combination of basicranial features: postglenoid process massive; posttympanic process enlarged, partially fused with paroccipital process; paroccipital process slender and slightly longer than posttympanic process. Differs from other rhinocerotoids except paraceratheriines in having posterior portion of cranium (from the postglenoid process to the occipital condyle) long, about 25% of the whole length of cranium. Differs from other rhinocerotoids with combination of features of anterior dentition: three upper/lower incisors conical and subequal in size with tight arrangement; canines stubby, distinctively larger than incisors; and diastema short.

Forstercooperia Wood, 1938

Type species: *Forstercooperia totadentata* Wood, 1938.

Included species: The type species, *Forstercooperia mazhuangensis* Qiu and Wang, 2007, and *Forstercooperia ulanshirehensis*, sp. nov.

Revised diagnosis: Large forstercooperiines with skull length about 455 mm and length of M1–M3/m1–m3 about 105–130 mm (table 1–3). Differs from *Pappaceras* in hav-

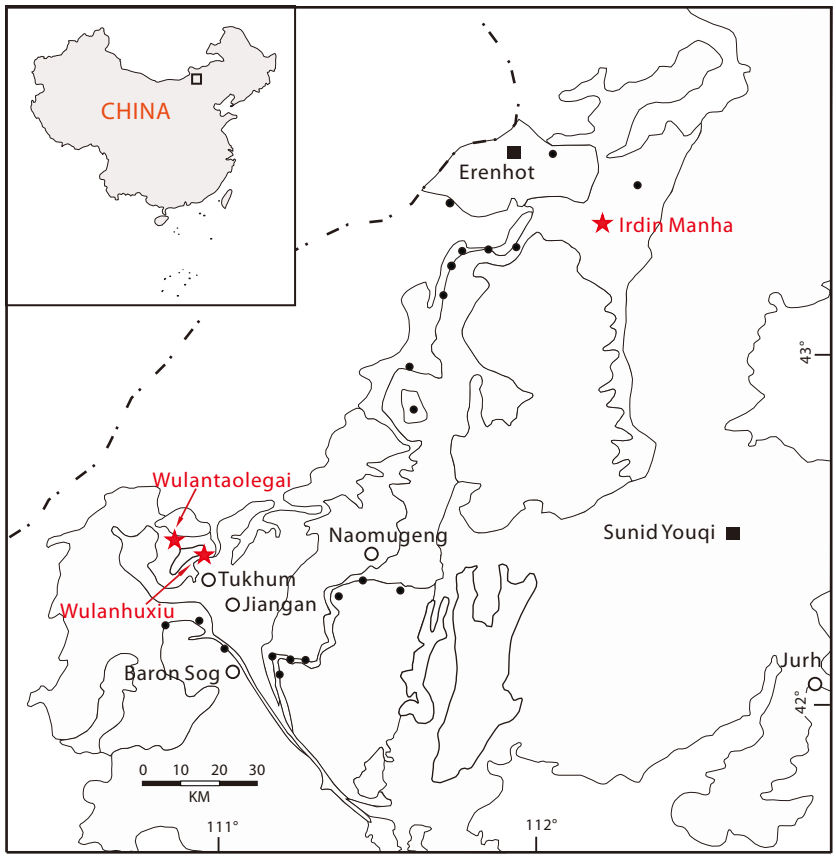

FIG. 1. Location of the main fossil localities in the Erlian Basin. Three localities (Irdian Manha, Wulantaolegai, and Wulanhuxiu), where the new specimens of *F. ulanshirehensis* were unearthed, are marked by red solid stars. Black solid circles represent other known fossil localities, solid squares denote cities or counties, and open circles denote towns and villages. This figure is modified from Wang et al., (2010).

ing a larger body size (the length of molar series greater than 100 mm), a transversely narrower postglenoid fossa with a well-developed median ridge separating two articular facets, sagittal crest distinct, occipital condyle comparatively more enlarged, dentition complete; I2 slightly larger than I1 and I3, canines stout and rounded at base; P2 premolarized with protocone and hypocone slightly separated; M3 triangular in occlusal outline along with the absence of metacone and ectoloph; tooth crowns of lower incisors nearly symmetric with distinct mesial and distal flanges, i2 larger than i1 and i3; and talonids of p3–4 elongate with the presence of entoconid.

***Forstercooperia ulanshirehensis*, sp. nov.**

Holotype: A nearly complete cranium (AMNH 21608) (figs. 2–4).

Referred specimens: A pair of complete mandibles (IVPP V20155) (figs. 5, 6), a fragmentary maxilla with P3–M3 (IVPP V20154) (figs. 7A, 7B); a fragmentary mandible with the

TABLE 1. Measurements of cranium of *Forstercooperia ulanshirehensis* (mm). H = height; L = length; Max = maximum; W = width.

Cranium	AMNH 21608
Basilar L	420[a]
Profile L (= total length)	455 [a]
Occipital–postorbital process, L	236.0
Premaxilla–postorbital process, L	225 [a]
P1-condyle, L	376.0
Postglenoid process–condyle, L	96.5
Anterior end of orbital–nasal notch, L	117.3 [a]
Premaxilla–anterior end of orbital, L	185.5 [a]
Zygomatic, Max W	182 [a]
Palatine at P1, W	53.2 [a]
Palatine at M1, W	51.8 [a]
Palatine at M3, W	52.8 [a]
Postglenoid processes, Max W	131.5
Paroccipital processes, Max W	99.1
Occipital, H	120.5 [a]
Foramen magnum, Max W	24.9
Occipital condyles, Max W	76.3
Occipital condyle, H	42.9
Occipital condyle, W	35.9

[a] Approximate measurements.

lower canine and p1–4 (IVPP V20156) (figs. 7C, 7D), and a fragmentary mandible with p3–m3 (AMNH 22101) (fig. 8).

Etymology: The specific name *ulanshirehensis* refers to the Ulan Shireh Formation, in which AMNH 21608 was collected.

Horizon and locality: AMNH 21608 (field number, 613), Ulan Shireh Formation, Wulanhuxiu site (previously known as 8 miles north of Tukhum Lamasery) of Erlian Basin, Nei Mongol, China; AMNH 22101 (field number, 602), Ulan Shireh Formation, Wulantaolegai site (previously known as 4 miles north of Tukhum) of Erlian Basin, Nei Mongol, China; IVPP V20154, V20155, and V20156, Irdin Manha Formation, Irdin Manha site, Erlian Basin, Nei Mongol, China. Middle Eocene.

Diagnosis: Small species of *Forstercooperia*, the length of upper premolar series about 81 mm, about 25% smaller than that of *Forstercoopeia totadentata* (~108 mm), about 20% smaller than that of *Forstercooperia mazhuangensis* (~103 mm) (see appendix, tables 2–3). Upper premolars transversely slightly narrower. Protocone and hypocone of P2 barely separate, metaloph of P2 narrow and posterolingually oriented. Metalophs (metaconules) of P3–4 short. Entoconid of p4 present.

TABLE 2. Measurements of upper dentition of *Forstercooperia ulanshirehensis* (mm). L = length; W = width.

	AMNH 21608		IVPP V20154
	Left	Right	Right
P1 L	17.6		
P1 W	11.9		
P2 L	18.0	19.0 [a]	
P2 W	17.3		
P3 L	24.6	23.4 [a]	21.3 [a]
P3 W	25.8	27.0 [a]	29.2 [a]
P4 L	25.4	23.8 [a]	26.8
P4 W	31.3		34.4
M1 L	36.5	36.1 [a]	38.5
M1 W	35.9		34.8
M2 L	39.9	39.3 [a]	47.0
M2 W	43.3	41.3 [a]	42.6
M3 L	33.3	32.6	41.1
M3 W	41.0	38.5 [a]	
P1–4 L	81.4		
M1–3 L	106.7	104.2 [a]	123.0
P1–M3 L	177.8		
Diastema between C-P1, L	30.2	29.7 [a]	

[a] Approximate measurements.

Description

AMNH 21608 is well preserved except for the anterior portion of premaxilla and nasal, and the zygomatic arch (figs. 2–4). In lateral view (fig. 2), the dorsal profile is fairly flat, characteristic of a dolichocephalic cranium. The premaxilla is nearly completely damaged, and the alveoli of the upper canines represent the anterior tip of the preserved cranium. The rostral portion of the nasal is not preserved, and in anterior view, the nasal is dorsoventrally thin with the cross section platelike. The lateral border of the nasal smoothly curves lateroventrally to meet the maxilla with the facial exposure of the nasal narrow. The suture of the nasal and maxilla is almost horizontal. The maxilla is large and high, and trapezoidal in outline in lateral view. Above the maxillary diastema (between the alveoli of the upper canines and upper premolars), the lateral surface of the maxilla is slightly concave. The preorbital fossa is present, shallow and smooth on the lateral surface. The infraorbital foramen is a distinctive and large opening, situated above P3. The maxilla posteriorly contacts the zygomatic and lacrimal by forming a nearly vertical suture on the lateral surface. The postorbital process of the frontal is well developed, situated above the posterior border of M3. The dorsal roof of the orbital region is formed by the nasal extended posterolaterally and the wide frontal. The lacrimal has

TABLE 3. Measurements of mandible and lower dentition of *Forstercooperia ulanshirehensis* (mm). H = height; L = length; W = width.

	IVPP V20155		IVPP V20156		AMNH 22101
i1-condyle, L	421.0				
p1-mandibular angle, L	364.0				
Mandible at the condyle, H	178.0				
Mandible at the coronoid process, H	217.0 [a]				
Horizontal ramus at p1, H	88.5				
Horizontal ramus at m1, H	97.3				
Symphysis, L	96.4				
	Left	Right	Left	Right	Left
i1 L	11.7	11.6			
i1 W	16.0	17.1			
i2 L	13.7	13.7			
i2 W	18.5	16.7			
i3 L					
i3 W		14.6 [a]			
c L	20.0	19.6	20.0	20.4	
c W	14.3	15.0	16.6	16.9	
p1 L	19.0	19.4	17.0	17.2	
p1 W	10.4	10.6	10.6	11.0	
p2 L	18.6	19.0	20.0	19.6	
p2 W	11.0	10.8	13.8	13.6	
p3 L	25.2	25.0	24.0	21.5 [a]	23.3 [a]
p3 W	14.5	14.2	15.0 [a]	16.8 [a]	15.4 [a]
p4 L	29.0	28.6		27.3	29.4
P4 W	17.2	16.8		20.0	17.4
m1 L	35.3	35.5			31.0
m1 W	22.6	22.4			22.2
m2 L	43.3	42.8			37.4
m2 W	26.0	27.2			25.4
m3 L	46.1	44.1			37.9
m3 W	27.5	25.5			24.8
p1-4 L	92.8	91.6		85.0	
m1-3 L	129.5 [a]	125.4 [a]			110.5
p1-m3 L	219.0 [a]	218.0			
Diastema between c-p1, L	34.9	35.2 [a]		33.9 [a]	

[a] Approximate measurements.

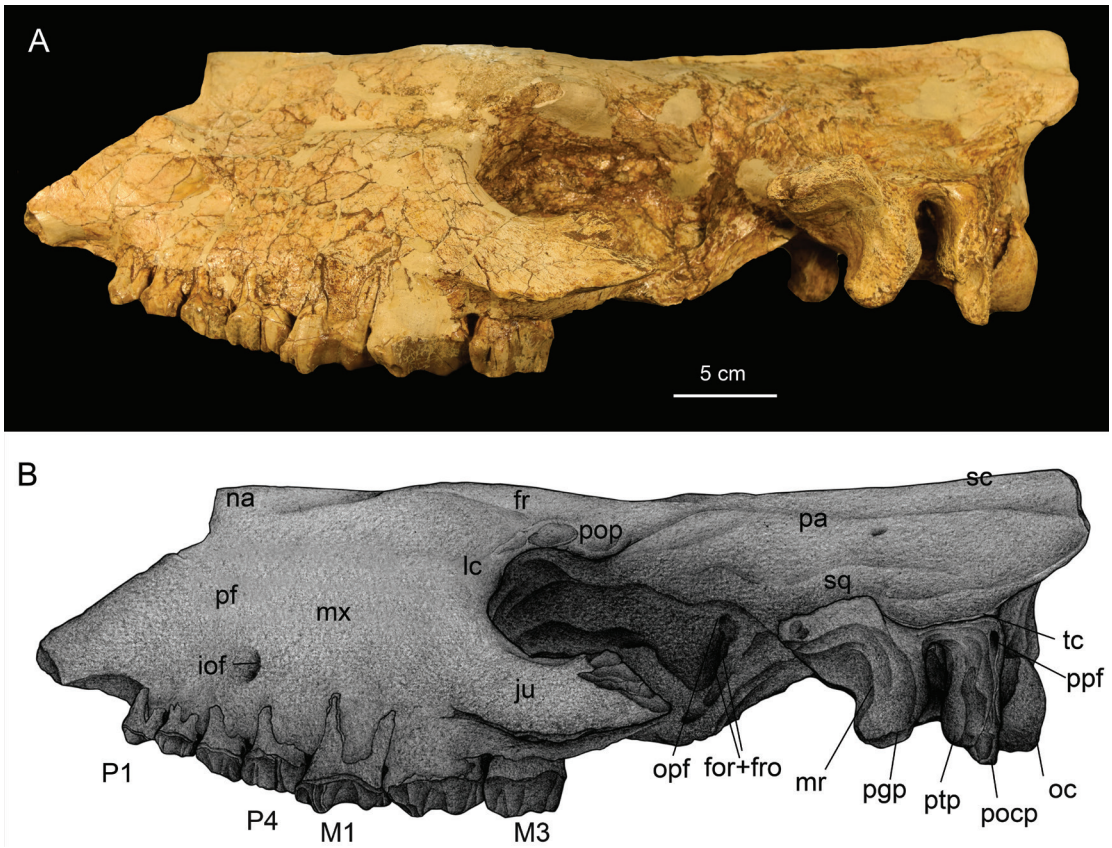

FIG. 2. Cranium of *F. ulanshirehensis* (AMNH 21608) in lateral view. Abbreviations: **for,** foramen orbitale; **fr,** frontal; **fro**, foramen rotundum; **iof,** infraorbital foramen; **ju,** jugal; **lc,** lacrimal; **mr**, median ridge of postglenoid process; **mx,** maxilla; **na,** nasal; **oc,** occipital condyle; **opf,** optic foramen; **pa,** parietal; **pf**, preorbital fossa; **pgp,** postglenoid process; **pop**, postorbital process; **pocp,** paroccipital process; **ppf,** posttympanic-paroccipital foramen; **ptp,** posttympanic process; **sc**, sagittal crest; **sq,** squamosal; **tc**, temporal crest.

a rough surface with some damages and its anterior and ventral sutures are identified, nearly forming a right angle. The zygomatic contacts the lacrimal nearly at the middle point of the anterior orbital margin. The zygomatic is flat on the lateral surface, rough on the ventral surface, and shows a well-developed ridge along the ventrolateral margin. The zygomatic arch is not preserved, and rises slightly posteriorly. The poor preservation of the orbital region makes it hard to accurately identify particular foramina and fissures, except the one regarded as the optic foramen on the left side (fig. 2). Ventral to the optic foramen is the foramen orbitale and the foramen rotundum, but the boundary of the two openings is not preserved. Laterally, the zygomatic process of the squamosal is dorsoventrally thin. The zygomatic arch is badly damaged on the both sides. The glenoid fossa is widely open. The squamosal ventrally bears the postglenoid process, which possesses two articular facets divided by a ridge, the medial facet facing anteriorly and the lateral facet facing anterolaterally. Posteriorly, the posttympanic process is widely separated from the postglenoid process. The posttympanic process is partially fused with the paroccipital process posteriorly, and the former is robust and anteroposteriorly

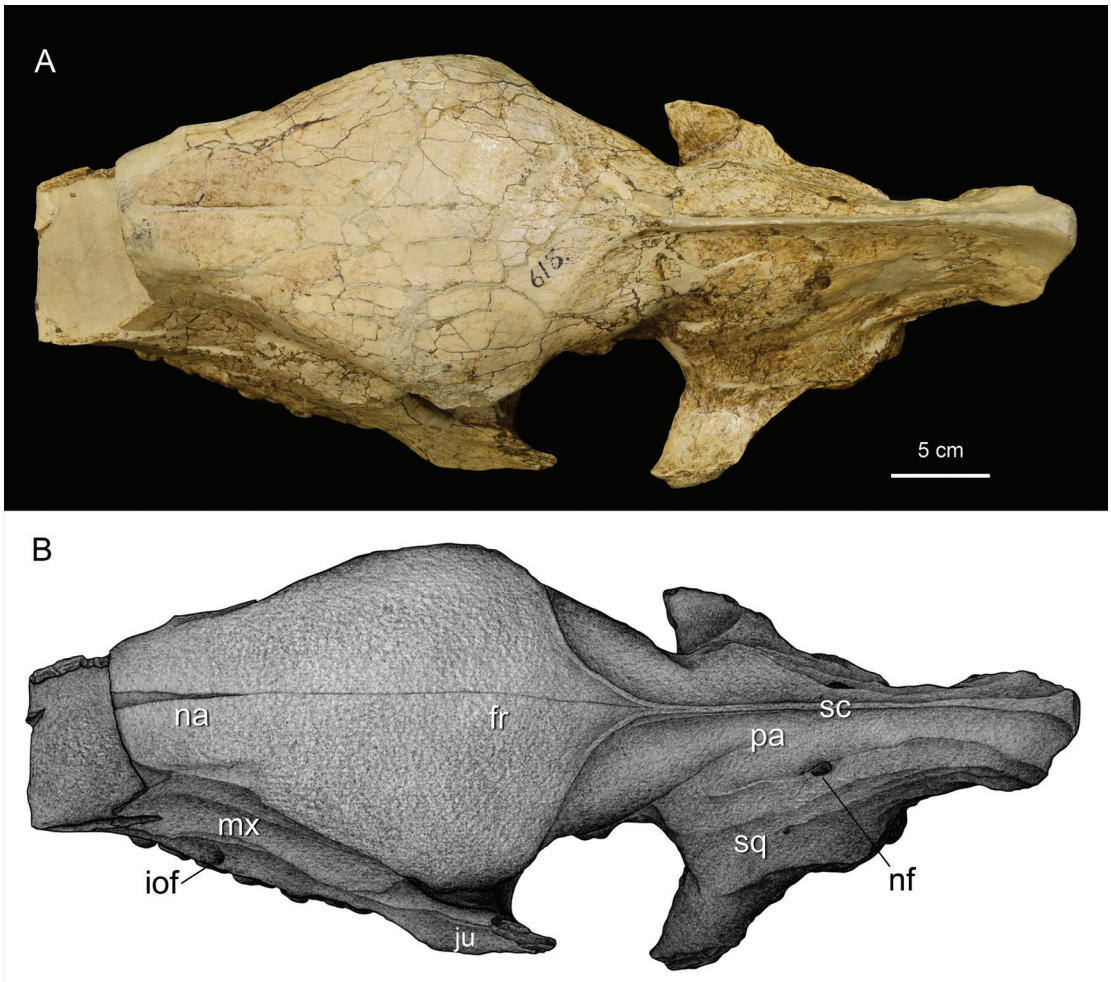

FIG. 3. Cranium of *F. ulanshirehensis* (AMNH 21608) in dorsal view. Abbreviations: **fr**, frontal; **iof,** infraorbital foramen; **ju,** jugal; **mx**, maxilla; **na,** nasal; **nf**, nutrient foramen; **pa,** parietal; **sc,** sagittal crest; **sq,** squamosal.

thickened, whereas the latter is more slender, slightly longer and nearly vertically directed. Lateral to the posttympanic process and the paroccipital process is the posttympanic-paroccipital foramen with a large opening at the dorsal extremity (equivalent to mastoid foramen) (fig. 2) (Holbrook, 2001). The occipital extends posteriorly beyond the level of the occipital condyle.

In dorsal view (fig. 3), the tip of the nasal might extend anteriorly more than the level of the upper canine, judging from the width of the posterior part of the nasal. The nasal increases in width posteriorly, and extends lateroposteriorly to the anterior part of the postorbital process, contacting the frontal at the level of the anterior border of the orbit. The frontal contributes to the widest part of the cranium at the level of the postorbital process, and decreases in width posteriorly. The frontoparietal crests gradually rise from the postorbital process posteriorly, and fully merge together slightly anterior to the suture of the frontal and parietal (~10 cm

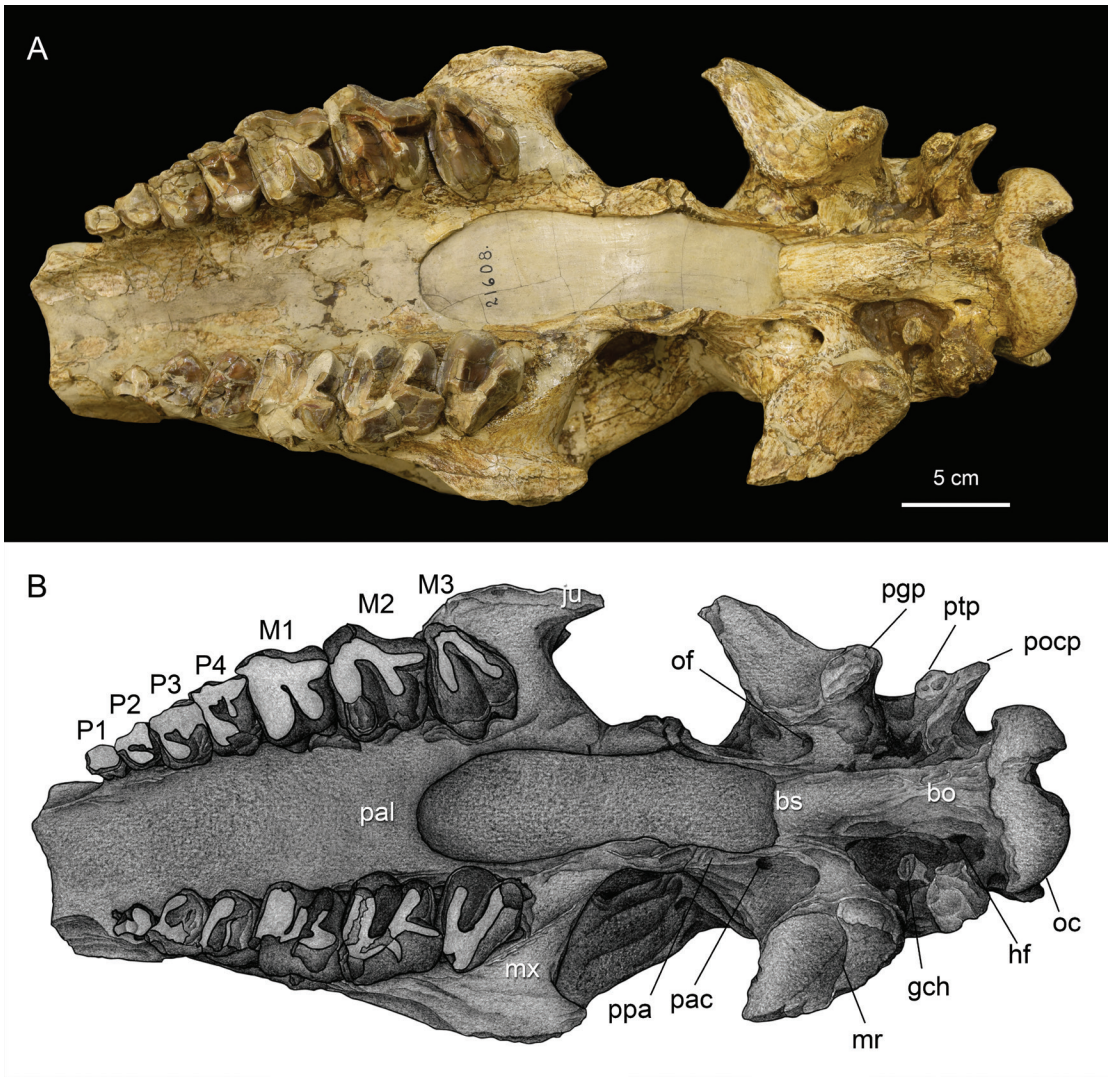

FIG. 4. Cranium of *F. ulanshirehensis* (AMNH 21608) in ventral view. Abbreviations: **bo,** basioccipital; **bs,** basisphenoid; **gch,** partial great cornu of hyoid; **hf,** hypoglossal foramen; **ju**, jugal; **mr,** median ridge of postglenoid process; **mx,** maxilla; **oc,** occipital condyle; **of,** oval foramen; **pac,** posterior opening of the alisphenoid canal; **pal,** palatine; **pgp,** postglenoid process; **pocp,** paroccipital process; **ppa**, pterygoid process of alisphenoid; **ptp,** posttympanic process.

anterior to the posterior tip of the cranium) forming the well-developed sagittal crest. The sagittal crest slightly elevates posteriorly. The dorsal roof decreases in width from the postorbital process posteriorly. The posterior part of the cranium is clearly narrower, with the dorsal profile steep and slightly higher than the anterior, especially the parietal and occipital regions. There are at least seven nutrient foramina present on the dorsal surface of the parietal and squamosal with some variation in size, of which a pair of nutrient foramina are nearly symmetrically positioned along the sagittal crest and distinctively larger than the others.

In ventral view (fig. 4), the anteriormost part of the cranium is the large upper canine alveoli. Posteriorly, the diastema between the upper canines and upper premolars is short (~3 cm), and the ventral margin of the diastema is slightly concave. The horizontal part of the palatine between the cheek-teeth rows is slightly concave rather than flat with a smooth ventral surface. The anterior process of the palatine is not preserved, and the number of the incisive foramina is unknown. The posterior border of the palatine is located at the level of the posterior border of M2. The suture between the maxilla and the jugal is distinct, nearly parallel to the long axis of the cranium. A short ridge that is similar to the facial crest rises from the anterior suture between the maxilla and jugal, and anteriorly shrinks at the level of the M2. Ventrally, the pterygoid process of the alisphenoid and the pterygoid process of the palatine form a small concave plate with an uneven ventral surface potentially for muscular attachment of the m. pterygoideus. Posteriorly, the pterygoid process of the alisphenoid bears a sharp ventral margin. Lateral to the alisphenoid, there are two large openings, of which the anterior is the posterior opening of the alar canal that opens posteriorly, while the posterior is the oval foramen that opens anteriorly. The cavity of the posterior choana has been fully filled by layers of plaster during preparation, and so it is not possible to identify many details in this region (e.g., the vomer and sphenoid). The posterior part of the cranium is elongate (the length from the postglenoid process to the occipital condyle ~96.5 mm). The postglenoid process is massive and transversely narrow. The glenoid fossa is extensive with a distinct component on the ventral surface of the zygomatic process of the squamosal. There is no sign of the postglenoid foramen posterior to the postglenoid process. On the left side, the posttympanic process is distinctly inflated and anteroposteriorly thickened despite the damage to the ventral part. Posteriorly, the paroccipital process is slender, transversely wider and anteroposteriorly thinner than the posttympanic process, and the two processes are partially fused. The basioccipital is well developed and ventrally bears a distinctive basilar process. Posterior to the basilar process is a distinct median ridge on the ventral part of the basioccipital. The hypoglossal foramen is large and medial to the paroccipital process. A fragmentary bone that is connected with the base of the temporal bone on the right side is the posterodorsal part of the great cornu of the hyoid bone. The foramen magnum has an oval outline in posterior view, formed by a pair of large occipital condyles. The occipital profile is nearly vertical. Dorsally, the occipital crest is damaged.

The whole mandible of IVPP V20155 is well preserved, but slightly distorted nearly in the middle and slightly damaged at the right condyle (figs. 5, 6). The mandibular symphysis is short, narrow, and dorsoventrally deep, making the anterior dentition tightly arranged. The posterior border of the mandibular symphysis is situated at the boundary between p1 and p2. The diastema between the lower canine and p1 is rather short (34.5 mm) and transversely constricted, forming a distinctive lateral depression. The horizontal ramus is slender with a slightly convex ventral border. On the left side, there is a large mental foramen below the anterior border of p1. On the right side, there are four mental foramina: the anterior one situated below i3, the middle two close to each other lying below the diastema, and the posterior one situated below p2. The lateral surface of the horizontal ramus is smooth, but slightly concave below p1–p4. The mandibular angle is rounded with the ventral border of the horizontal ramus

FIG. 5. Mandibles of *F. ulanshirehensis* (IVPP V20155) in occlusal view. Abbreviations: **cdp**, condylar process; **crp**, coronoid process; **pcp**, postcotyloid process.

slightly convex, and the posterior border of the ascending ramus nearly vertical. Both the lateral and medial surfaces of the mandibular angle are considerably rough, of which the latter is more concave than the former. Laterally, ventral to the coronoid process is the masseteric fossa, represented by a shallow depression with a nearly triangular outline. Medially, the mandibular foramen is large, situated slightly lower than the alveolar border and vertically below the coronoid process. The coronoid process is inclined posteriorly at the top, and is higher than the mandibular condyle. The condyle is quite high above the occlusal plate of the cheek teeth. The surface of the condyle is rough and fairly flat dorsally. Posterior to the condyle, the postcotyloid process is rather weak, showing a convex posterior margin of the mandible in lateral view. The mandibular incision is broad and opens posteriorly.

The dental formula is ?·1·4·3/3·1·4·3. The dentition of AMNH 21608 (fig. 4) and AMNH 22101 (fig. 8) are moderately worn, whereas the dentitions of IVPP V20154 (figs. 7A, 7B), IVPP V20155 (figs. 5, 6), IVPP V20156 (figs. 7C, 7D) are less worn.

The P1 is preserved only on the left side of AMNH 21608. This tooth is double rooted and heavily worn. Its outline is nearly trapezoidal with the length larger than the width in occlusal

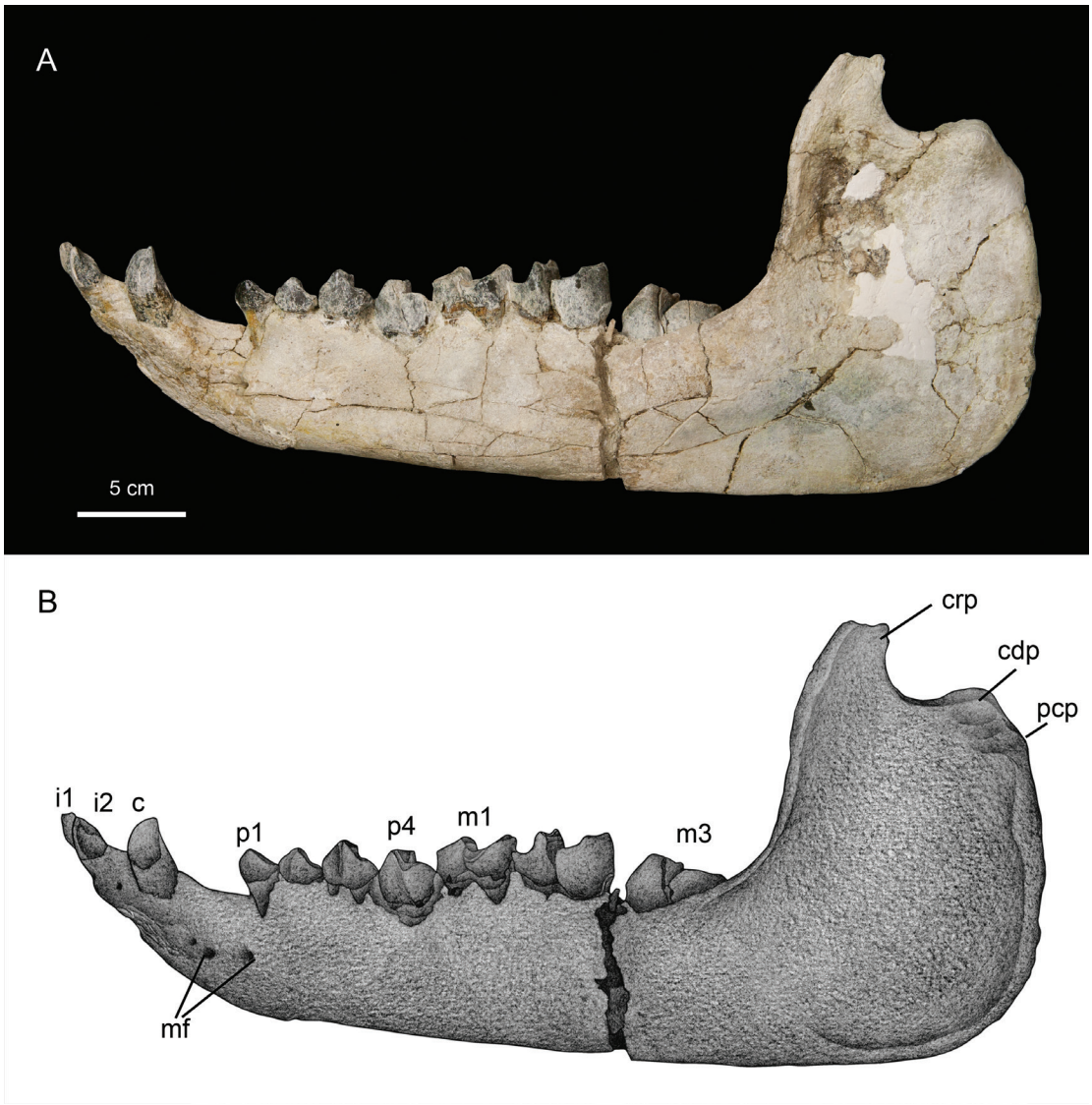

FIG. 6. Mandibles of *F. ulanshirehensis* (IVPP V20155) in lateral view. Abbreviations: **cdp**, condylar process; **crp**, coronoid process; **mf**, mandibular foramen; **pcp**, postcotyloid process.

view. The paracone is the largest and highest portion of the tooth. The cingulum is distinct and continuous in the lingual and labial side. P2 is larger than P1, nearly quadrate in occlusal view with the protoloph well developed and the metaloph (or metaconule) weak. The protoloph of P2 is oriented anterolaterally to contact the ectoloph with a notch at the base of the paracone. The metaloph is short and extends posterolingually to contact the protoloph. From the wear surface, the protocone and hypocone of P2 are slightly separate, because there is a small isolated wear facet immediately posterior to the posterolingual margin of the protoloph, where the small hypocone is located but that facet becomes invisible after moderate or heavy wear.

Despite the damage to the ectoloph, the paracone and metacone of P2 is nearly equal in height, and the parastyle fold is shallow. The cingulum of P2 is well developed at the lingual, anterior, and posterior bases. The P3 is similar to P2 in basic structure, but larger in size. The ribs of the paracone and metacone are distinct on the lateral side of the ectoloph. The protoloph of P3 is more robust than that of P2, occupying most of the lingual space of tooth crown. The metaloph of P3 is weak and short, and extends nearly transversely. In IVPP V20154, the metaloph of P3 contacts the protoloph, but it is not the case in AMNH 21608, in which there remains a tiny gap between the protoloph and the short metaloph. The postfossette of P3 (space posterior to the metacone) is broad compared to those of P1–P2. The cingulum of P3 is similar to that of P2, but absent on the buccal side. The P4 is rectangular in occlusal outline with its width greater than its length. The parastyle is more distinct than in P1–P3, and transversely pinched, forming a deep parastyle fold with the paracone. A weak crista is present in the lingual side of the ectoloph of P3–P4. The protoloph of P4 is massive on the lingual side, and sharply decreases in width buccally to contact the ectoloph. The metaloph of P4 is slightly longer and more robust than that of P3, and transversely extends to contact the protoloph. The postfossette of P4 is relatively transversely wider than that of P3. The cingulum of P4 is similar to that of P3.

The M1 is heavily worn and nearly quadrate in occlusal outline with distinct parastyle and parastyle folds on the buccal wall. The paracone rib is well developed, while the metacone rib is faint. The M2 is similar to M1 in basic structure, but distinct from the latter in having a larger size, relatively more elongated and lingually oriented ectoloph, and shorter metaloph. The M3 is distinguished from M1–2 with a nearly triangular outline. The parastyle of M3 is slightly weak, situated at the anterolateral base and slightly warped toward the lingual side. The ectoloph of M3 is completely fused with the metaloph. The metacone of M3 can be traced by the presence of a slightly concave posterior surface of the metaloph in AMNH 21608, but it is completely absent in IVPP V20154. The cingulum of the upper molars is distinct at the anterior, lingual, and posterior bases, and absent on the buccal side.

The lower incisors are preserved only in IVPP V20155. The left i3 is not preserved and the right i3 is damaged at the mesial side. Three incisors are tightly arranged nearly longitudinally. The lower incisors are generally subequal in size, but the i2 is slightly larger than the i1 and i3. The occlusal outlines of the lower incisors are similar in having somewhat conical and nearly symmetric crowns with distinct mesial and distal flanges. Each incisor bears a blunt ridge on the distal (lingual) wall of the tooth crown. The first lower incisor is relatively procumbent with its tooth crown more asymmetric than in i2 and i3. The crown of i2 extends much more laterally (transversely) than anteroposteriorly, and possesses a triangular outline in posterior view. The distal flange is well developed in i2, while slightly weaker in i1 and narrower in i3. The right i3, represented by only the distal portion, is similar to i2 in outline, except it aligns nearly anteroposteriorly.

The lower canine is well preserved on both sides of IVPP V20155 and V20156. There is no distinct diastema between the i3 and lower canine. This tooth is conical, rather stubby and much larger than lower incisors with its base more rounded, especially in IVPP V20156. Anteriorly, a distinct flange smoothly extends from the top to the mesial (lingual) base of the tooth

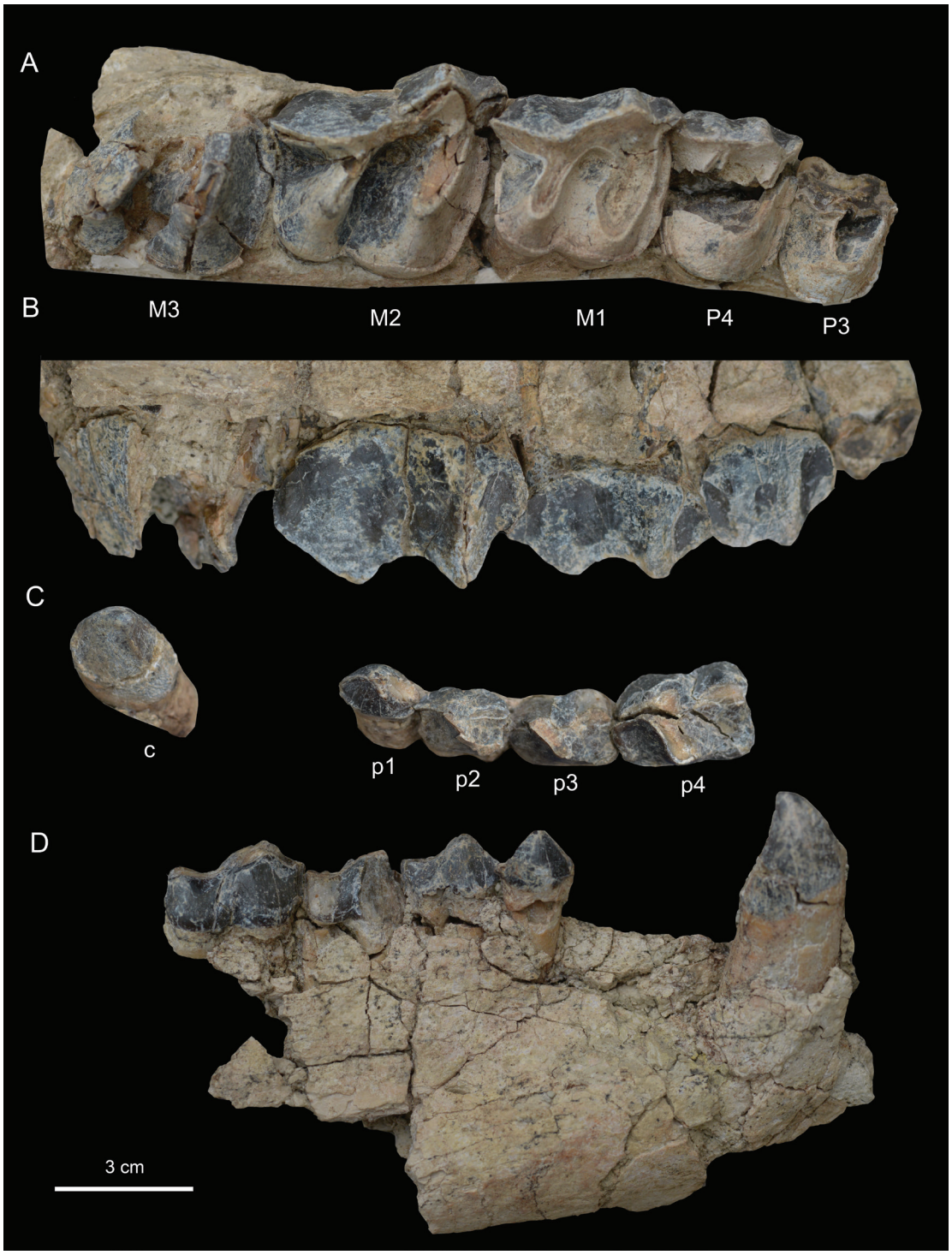

FIG. 7. Dentition of *F. ulanshirehensis* in lateral and occlusal view. **A**, IVPP V20154 in lateral view; **B**, IVPP V20154 in occlusal view; **C**, IVPP V20156 in occlusal view; **D**, IVPP V20156 in lateral view.

crown. Posteriorly, this tooth bears two flanges, which descend from the tip to the base of the tooth crown, forming a triangular facet on the distal side. The ridges are evident in IVPP V20155, but slightly weaker in IVPP V20156. The cingulid of the lower canines at the base is weak, and present only at the anterior base.

The p1 is double rooted. It is roughly bladelike in occlusal view, but wide with a convex lateral wall. The trigonid of p1 is simply structured and mainly comprises a weak paraconid and a distinct protoconid, which are nearly anteroposteriorly arranged, making the trigonid basin shallow. The paralophid is represented by a very short ridge. The talonid is short, and its short hypolophid forms a shallow talonid basin. The cingulid is weak and present only at the anterolingual and posterolingual base. In IVPP V20155 the anterior ridge extends more anterolingually, deepening the trigonid basin more than in IVPP V20156.

The p2 has a nearly rectangular base in occlusal view, and is larger than p1. The trigonid of p2 is wider, and possesses a larger protoconid than that of p1. The protolophid of p2 anterolingually extending makes the trigonid basin a little deeper than that of p1. The paralophid of p2 is short and the metaconid is not distinctly separated from the protoconid. The trigonid of p2 is higher, longer, and narrower than the talonid. The talonid is primitive with a short and lingually oriented hypolophid and absent entoconid. The talonid is surrounded by a short ridge around the posterior base of the talonid. The cingulid is distinct anteriorly and posteriorly, and absent laterally and lingually in p2. In IVPP V20156, the p2s are slightly damaged on the lingual side. In IVPP V20155, the metalophid is oriented relatively posterolingually.

The p3 is basically similar to p2, but larger. It also differs from p2 in having a longer paralophid and a higher hypoconid in the talonid. The metalophid of p3 is oriented more transversely than that in p1 and p2. The trigonid of p3 is slightly shorter than the talonid, in which the hypoconid is much higher than that of p2. Both the trigonid and the talonid of p3 are distinctly deeper and wider than those of p2. The cingulid of p3 is well developed at the anterior and posterior bases, continuous at the buccal base but absent on the lingual side.

The p4 is larger than p3, but with blunter cusps and lophs. The paraconid of p4 is located more lingually and the metalophid of p4 is oriented more transversely than in p1–3, making the trigonid U-shaped and the trigonid basin deep. The talonid of p4 is almost equal in length with the trigonid. Compared with p1–p3, the remarkable difference is the presence of the entoconid in p4. The entoconid of p4 is still weak and isolated from the hypoconid, which is much higher in the talonid. The cingulid of p4 is the same as that of p3.

The m1 is well preserved with intermediate abrasion in IVPP V20155 and heavy abrasion in AMNH 22101. This tooth is distinctly larger than lower premolars. The trigonid of m1 is wide with the paralophid long and laterally extended, and the protolophid of m1 more anterolingually oriented. The metalophid of m1 is strong and extends slightly posterolingually. The talonid of m1 is wide with a well-developed hypolophid ("cristid obliqua") and entolophid ("hypolophid"). The entoconid of m1 is a little more posteriorly displaced than the hypoconid of m1. The hypolophid contacts the entolophid with an oblique angle. The cingulid of m1 is distinct anteriorly and posteriorly, and absent lingually, whereas the buccal cingulid is continuous, but slightly reduced at the base of the protoconid and hypoconid. The m2 is basically

FIG. 8. Dentition of *F. ulanshirehensis* in occlusal and lateral view (AMNH 22101). **A**, occlusal view; **B**, lateral view.

similar to m1, but larger than the latter. The m2 is less worn in occlusal view than m1. Its trigonid is longer than that of m1. The trigonid of m2 as well as that of m1 slightly increase in width posteriorly. The m3 is similar to m2 in crown outline. The m3s have not completely erupted in IVPP V20155. The cingulid of m2–3 is roughly the same as that of m1, except that the posterior cingulid is more distinctive in m3.

COMPARISON AND DISCUSSION

Comparison within Forstercooperiiines

The new specimens display characteristic features of Forstercooperiinae, such as the conical and nearly equal-sized lower incisors, large and stubby canines, primitive upper and lower premolars, and large size (Radinsky, 1967; Lucas et al., 1981; Lucas and Sobus, 1989). Specifically, the new specimens are unequivocally referable to *Forstercooperia* rather than *Pappaceras*, given the derived upper and lower premolars, particularly P2 and p4, larger body size (fig. 9) and younger age (Irdinmanhan). But they are distinguishable from the specimens of *Forstercooperia totadentata* and *Forstercooperia mazhuangensis* primarily based on the dental morphology, such as smaller size (fig. 9), primitive P2, short metalophs of P3–P4, and weak entoconid of p4. Consequently, we establish a new species, *Forstercooperia ulanshire-*

hensis, on the basis of these specimens, which is the third and best-known species of *Forstercooperia*. Besides the new species, *Forstercooperia* includes two species: the type species *F. totadentata* Wood 1938, which is represented by a considerably large, fragmentary cranium (AMNH 20116), and *Forstercooperia mazhuangensis* Qiu and Wang 2007, which is represented by a pair of fragmentary maxillae and mandibles (IVPP V5072). The new species, *F. ulanshirehensis*, is distinguished from *F. totadentata* and *F. mazhuangensis* by dental morphology (mainly the upper and lower premolars) and its smaller size. It is similar to *F. totadentata* (AMNH 20116) with the presence of large upper canines (based on the large alveoli of upper canines), complete upper premolars (P1–4), short diastemata, a shallow preorbital fossa, transversely wide P4, distinct crista, and straight metaconules of P3–4. But *F. ulanshirehensis* differs from *F. totadentata* in having transversely slightly narrower P2–3, a weak hypocone on P2, less-developed ribs of the upper premolars, and short metalophs of P3–4. In terms of size, *F. ulanshirehensis* is about 25% smaller than *F. totadentata* with the length of upper premolars about 81.4 mm for *F. ulanshirehensis* and about 108 mm for *F. totadentata* (fig. 9, table 2). *F. ulanshirehensis* is distinguishable from *F. mazhuangensis* with the short and posterolingually oriented metaloph of P2, transversely straight metaloph of P4, presence of entoconid of p4, and a smaller size (the length of P1–4 ~103 mm for *F. mazhuangensis*, ~20% larger than *F. ulanshirehensis*) (fig. 9, table 2).

The cranial features of *F. ulanshirehensis* display a derived condition within forstercooperiines. *F. ulanshirehensis* (AMNH 21608) shares primitive cranial structures with *Pappaceras*, such as a shallow preorbital fossa, high maxilla, wide frontal, greater ratio of the length of basal cranium to skull length, enlargement of posttympanic process, and the presence of posttympanic-paroccipital foramen and large occipital condyles. Compared with the well-preserved specimen of *Pappaceras meiomenus* (IVPP V20254) (Wang et al., 2016), *F. ulanshirehensis* is distinctively different in its (1) larger size, (2) enlarged occipital condyles, and (3) longer distance between the postglenoid process and the occipital condyle, which is about 26% of the distance between P1 and the occipital condyle (table 1). These three features of *F. ulanshirehensis* are also characteristics of paraceratheriines (giant rhinos) (Qiu and Wang, 2007). The posttympanic process of *F. ulanshirehensis* is thicker than that of *P. meiomenus*. The infraorbital foramen and oval foramen appear to be considerably larger openings in *F. ulanshirehensis* than in *P. meiomenus*. In *F. ulanshirehensis*, the postglenoid process is transversely narrow, and divided by a more developed median ridge into two facets, facing anteriorly and anterolaterally respectively, whereas it is transversely broad and relatively flat with a weak median ridge in *P. meiomenus*. The basicranium is broken in the holotype of *P. confluens* (AMNH 26660). *F. ulanshirehensis* (IVPP V20155) has five large mental foramina, one from the left and four from the right, whereas only one mental foramen is present below the p1 in *P. confluens*. The ventral border of the mandible in *F. ulanshirehensis* is relatively horizontal, while *P. confluens* and *P. minuta* have ventral borders that are slightly convex along with the presence of a distinct vascular impression (Wood, 1963; Lucas et al., 1981). In addition, the mandible of *F. ulanshirehensis* differs from that of *Pappaceras* in having a nearly vertical posterior border of the ascending ramus and a more rounded mandibular angle.

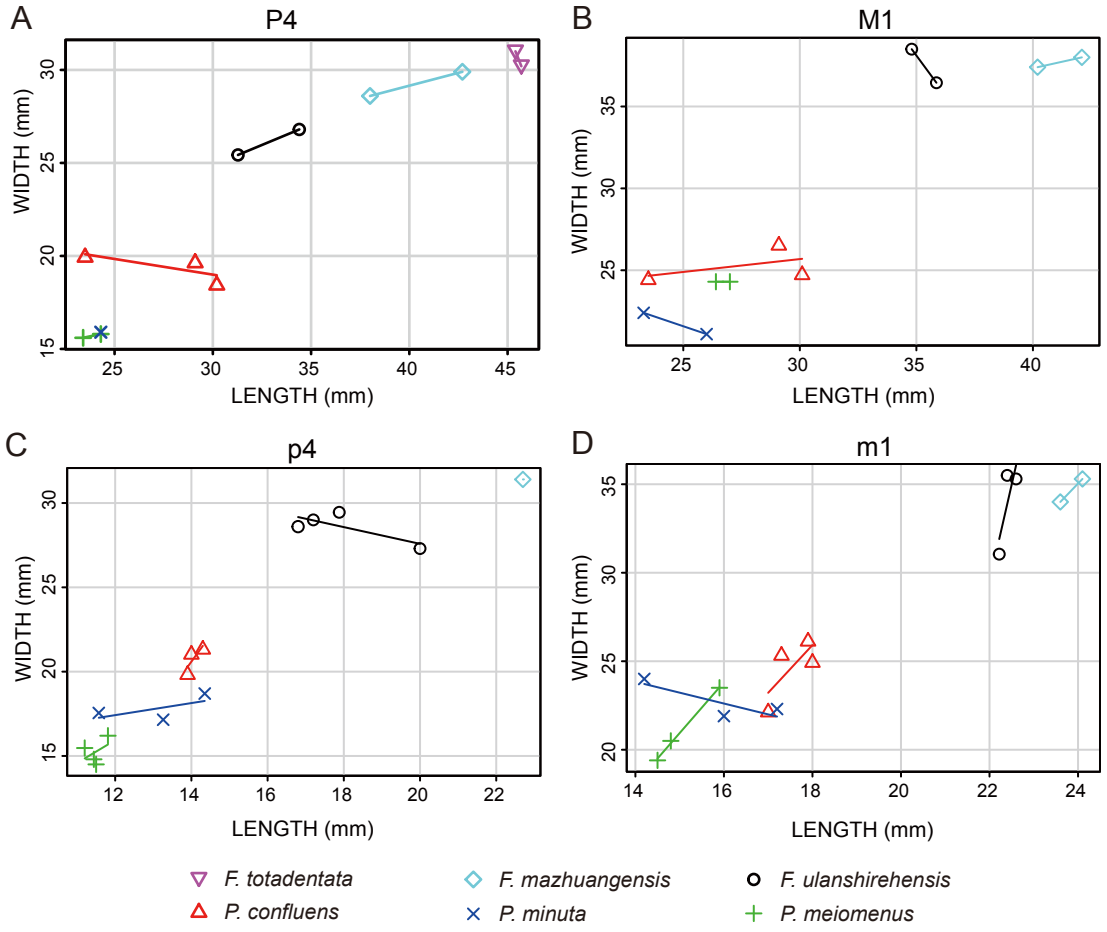

FIG. 9. Scatter plots of length vs. width across P4/p4 and M1/m1 of forstercooperiines. **A**, scatter plots of P4; **B**, scatter plots of M1; **C**, scatter plots of p4; **D**, scatter plots of m1.

F. ulanshirehensis provides the complete morphology of upper check teeth of *Forstercooperia*. The presence of P1 is consistent in *Forstercooperia*, including *F. ulanshirehensis*, and is different from that of *Pappaceras meiomenus*. The P2s of *Forstercooperia* show the rudimentary distinction of the protocone and hypocone in the lingual side, in contrast to the absence of a hypocone of P2 in *Pappaceras*. The structure of M1–2 in *F. ulanshirehensis* is similar to those of *P. confluens* and *P. minuta* in having relatively elongated ectolophs and lingually oriented metastyles. Another evident morphological difference in upper cheek teeth between *F. ulanshirehensis* and *Pappaceras* is that the metacone of M3 in *F. ulanshirehensis* is nearly absent, similar to that of *F. mazhuangensis*, forming a triangular occlusal outline. This is distinguished from *Pappaceras*, in which the M3 is either trapezoid in outline with the metacone lingually oriented and the ectoloph confluent with the metaloph in *P. confluens*, or almost quadrate with distinct metacones and metastyles for *P. minuta* and *P. meiomenus*. In addition, the antecrochets of M2–3 of *F. ulanshirehensis* are absent, more similar to *F. mazhuangensis*, *P. minuta*, and *P. meiomenus*, but different from *P. confluens*.

The morphology of the lower dentition of *Forstercooperia*, especially the anterior dentition, is comprehensively represented by the specimens of *F. ulanshirehensis* (IVPP V20155, V20156; AMNH 22101). It is confirmed from *F. ulanshirehensis* that the status of i1 of *Forstercooperia* is as follows: (1) i1 is almost equal to i2 in size, only slightly smaller than the latter; (2) the i1 is less conical and less symmetric in outline with distinct mesial and distal flanges than i2 and i3, similar to those of most primitive perissodactyls; (3) the i1s are closely situated medially and the roots rise much more vertically rather than anteriorly compared with those of paraceratheriines. The crowns of i2s in *F. ulanshirehensis* are more laterally extended, which is distinct from those of *P. confluens* and *P. minuta*. The lower canine of *F. ulanshirehensis* is immediately next to i3, similar to that of *P. confluens*, and it is considerably stubbier and larger than those of *Pappaceras*, especially at the base. Meanwhile, compared with the inferred characters of lower dentition of *F. totadentata* by Wood (1938), several differences that are revealed by the new mandibular specimens are in contrast to Wood's inference. *F. ulanshirehensis* has large lower canines, which are nearly equal in size to the upper canine based on the alveolus of upper canines, rather than smaller than the upper canines as inferred by Wood (1938). The p1 is primitive and large on both sides rather than the inferred reduced or absent condition. Within forstercooperiines, the reduction of p1 is present only in *P. meiomenus*. The p3 is relatively shorter (>30 mm) in *F. ulanshirehensis* than the inferred length in *F. totadentata*, and it is probably larger than 30 mm for *F. totadentata*. In contrast to Wood's inference that the p4 of *Forstercooperia* was shorter than p2–3, which corresponded to the transversely wide and longitudinally short P4, the p4 of *F. ulanshirehensis* is clearly longer than p2 and p3. Furthermore, the p4 bears an entoconid in *F. ulanshirehensis*, and this is a derived characteristic of *Forstercooperia* within forstercooperiines. On the basis of these characters, it is highly possible that the p4 (even p3) of *F. totadentata* may possess a distinctive entoconid, considering that the P2 in *F. totadentata* is more molarized than in *F. ulanshirehensis* with the protocone and the hypocone partially separate. The length of the lower premolar series is about 92 mm in *F. ulanshirehensis*, longer than Wood's inference (83 mm) for *F. totadentata*, which should be much larger.

Species-Level Taxonomy of Forstercooperiines

Excluding the new species, there are 12 species of forstercooperiines ("*Forstercooperia*") formally reported, and only six species are regarded as valid in the present study after examining all specimens formerly assigned to Forstercooperiinae. All species that were formally created in previous studies are listed here (invalid names marked by quotation marks): *Forstercooperia totadentata* Wood, 1938, *Pappaceras confluens* Wood, 1963, *Hyrachyus grandis* Peteson, 1919 ("*Forstercooperia grandis* Radinsky, 1967"), *Eotrigonias borissiaki* Beliayeva, 1959 ("*Forstercooperia borissiaki* Lucas et al., 1981"), "*Forstercooperia ergiliinensis* Gabounia and Dashzeveg, 1974," "*Forstercooperia shiwopuensis* Chow et al., 1974," "*Forstercooperia jigniensis* Sahni and Khare, 1973," "*Forstercooperia crudus* Gabounia, 1977," "*Forstercooperia minuta* Lucas et al., 1981," "*Forstercooperia huhebulakensis* Qi, 1987," *Imequincisoria mazhuangensis*

Wang, 1976 (*Forstercooperia mazhuangensis* Qiu and Wang, 2007), and *Pappaceras meiomenus* Wang et al., 2016. Currently, three species of *Forstercooperia*, *F. totadentata*, *F. mazhuangensis*, and *F. ulanshirehensis*, are regarded as valid, while *Pappaceras confluens* ("*Forstercooperia confluens*") has been resumed and *Pappaceras minuta* ("*Forstercooperia minuta*") has been regarded as a composite on the basis of the validity of *Pappaceras*. "*F. shiwopuensis*" has been accepted as a junior synonym of *F. totadentata* based on previous works (Lucas et al., 1981; Lucas and Sobus, 1989), with which we agree in the present paper. Another three species, "*F. borissiaki*," "*F. ergiliinensis*," and "*F. jigniensis*," have been correctly excluded from *Forstercooperia* (Lucas et al., 1981; Lucas and Sobus, 1989; Qiu and Wang, 2007). The type specimens of "*F. grandis*" have been assigned to *Uintaceras* by Holbrook and Lucas (1997); as a result, *F. grandis* is no longer a valid name.

The latest study of forstercooperiines erects *Pappaceras meiomenus* based on a complete cranium (IVPP V20254) (Wang et al., 2016). This specimen is distinguished by the loss of P1. It should be noted that the specimens assigned to *Pappaceras minuta* ("*F. minuta*") by Lucas et al. (1981) show a mixed condition on the reduction of P1/p1, which was interpreted as interspecies variation at the time. In the two type specimens of *P. minuta* (AMNH 26672), despite the lack of P1, a distinct alveolus for P1 on the fragmentary maxilla confirms its presence, while the p1 is hardly visible from the damaged mandible of a young juvenile individual due to poor preservation. Considering the completeness of premolar series in most primitive perissodactyls, the interpretation that regarded the absence of P1/p1 in *P. minuta* as intraspecific variation can be seriously challenged. Alternatively, it is proposed that the questionable specimens formerly assigned to *P. minuta* with the absence of P1/p1 are temporarily referred to *P. meiomenus*. These specimens include AMNH 26677, 107851, 107852, 107856 (see appendix). In other cases that cannot directly estimate the presence or absence of P1/p1 in a particular specimen, we are temporarily inclined to refer these specimens tentatively as *Pappaceras* sp. (including AMNH 26669, 26671, 107848, 107849). In addition, a juvenile left fragmentary dentary with deciduous p2–3 (AMNH F: AM 99662) has been regarded as an indeterminate species (Holbrook and Lucas, 1997). The specimens that involve taxonomic status changes are listed in the appendix. Accordingly, the content of three species of *Pappaceras* has been changed after the current revision.

The confusion of "*F. crudus*" was discussed and tentatively considered a nomen nudum in the revision work for forstercooperiines (Lucas et al., 1981). The specimens assigned to "*F. crudus*" are from the Sargamys Formation of the Zaissan Basin in Kazakhstan (Gabounia, 1977). Gabounia (1977) failed to provide a formal and detailed description of involved specimens in the original text, in which an isolated ?M2 and a fragmentary mandible with p2–m3 were referred to in the text as "figure 17" and "figure 19" respectively (Gabounia, 1977: 31). The plate on which the images appeared, however, were not labeled but figures, but rather were labeled alphabetically (so fig. 17 would correspond to q and fig. 19 to s); however, the caption describing the isolated ?M2 ("q" on pl. 1) was omitted for some reason (along with its scale) (Gabounia, 1977: 36), whereas the mandibular specimen ("s") was confusingly described as "*Forstercooperia* sp." in the caption (Gabounia, 1977: 36, pl. 1). Without a standard for ?M2 in the plate, it is hard to measure the size of this tooth accurately and assign it to any specific

genus, because it is similar to those of *Forstercooperia* and some hyracodontids in having a relatively elongated ectoloph, such as in *Prohyracodon* and *Epitriplopus*. As a result, it is not possible to confirm its affinity based on an incomplete and less characteristic M2, even if the size of this tooth could be determined in the future. In terms of the mandible specimen, Lucas et al. (1981) mentioned that the mandible is similar to *P. minuta* in size, but has derived p3–4 with distinct entoconids and relatively strong entolophids. In general, the derived features of lower premolars in the Zaissan specimen are distinctively in contrast to *Forstercooperia* and even to most of the Middle Eocene rhinocerotoids, which usually lack entolophids on p3–4. In addition, the cheek teeth of the Zaissan specimens were measured according to the plate, and the length of m1–3 is about 68.0 mm, which is remarkably smaller than that of *Forstercooperia*. Therefore, it seems unreasonable to assign this specimen to *Forstercooperia* under any circumstance. These specimens might be related to some derived hyracodontids based on dental morphology, and therefore, we suggest considering "*F. crudus*" as an indeterminate rhinocerotoid.

The species "*F. huhebulakensis*" is not a valid species of *Forstercooperia*. It was proposed that *F. huhebulakensis* occurred stratigraphically lower than "*F. confluens*" (Qi, 1987), but recent studies have suggested the argument is incorrect (Meng et al., 2007; Wang et al., 2010). Meng et al. (2007) and Wang et al. (2012) confirmed that the holotype (IVPP V5770) of "*F. huhebulakensis*" was unearthed from the "upper gray clays" of the Arshanto Formation in the Huheboerhe area, which is stratigraphically equivalent to that of *P. confluens*. Meanwhile, Qi (1987) failed to compare "*F. huhebulakensis*" with *P. minuta*, and he suggested that "*F. huhebulakensis*" was smaller than *F. totadentata*, and differed from *P. confluens* in having a "flatter and straighter" zygomatic arch, "flatter frontal and nasal bones" and M2–3 without anticrochets. Actually, the holotype of "*F. huhebulakensis*" has a characteristic M3 of *P. confluens* with the metacone lingually oriented and the ectoloph distinctively reduced. The length of M1–3 in "*F. huhebulakensis*" (79.7 mm) is slightly smaller (8%) than that of *P. confluens* (87.1 mm) and considerably smaller than that of *F. totadentata* (123.0 mm). The zygomatic and frontal of "*F. huhebulakensis*" are also similar to those of *Pappaceras* (*P. minuta* and *P. meiomenus*). Consequently, the holotype of "*F. huhebulakensis*" should be assigned to *P. confluens* as a relatively small individual, making "*F. huhebulakensis*" a junior synonym of *P. confluens*.

Furthermore, we agree with Qiu and Wang (2007) that "*Imequincisoria mazhuangensis* Wang, 1976" should be combined with *Forstercooperia mazhuangensis*. "*Imequincisoria mazhuangensis*" was created based on a pair of fragmentary maxillae, mandibles, and some isolated anterior teeth (IVPP V5072) (Wang, 1976). Among these materials, the maxillae and mandibles have been assigned to *F. mazhuangensis*, whereas the anterior teeth have been put into *Juxia micracis* Qiu and Wang, 2007 (Qiu and Wang, 2007). The morphology of upper premolars in *F. mazhuangensis* is more similar to that of *Forstercooperia* than *Juxia*; in particular, the metalophs of P2–3, though relatively well developed, are distinctively transversely straight, the protocone and metacone of P2 are barely separate and the P4 is transversely wide in *F. mazhuangensis*. With regard to the fragmentary mandibles, the entoconid is absent in the lower premolars of *F. mazhuangensis*, primitively similar to *Pappaceras*, but distinct from *Juxia* in which the entoconid is usually pres-

ent in p3–4. The anterior dentition that has been assigned to *J. micracis* is, though generally conical in outline, clearly smaller and narrower than those of *F. ulanshirehensis*, and considerably varies in size, which links this specimen to *Juxia* rather than forstercooperiines. In addition, Qiu and Wang (2007) considered that the large-sized postcranial specimens (carpals and metacarpals) (IVPP V5074.1-8) from the Wucheng basin formerly assigned to *Imequincisoria* (?) sp. would be referable to *F. mazhuangensis*, mainly because of its larger size and tridactyl manus. Given that there remains no known unequivocal postcranial specimens of forstercooperiines, the taxonomy of the mentioned specimens (IVPP V5074.1-8) is in need of further discussion and revision. Namely, these specimens are tentatively regarded as indeterminate rhinocerotoid, and not used as coding resources of forstercooperiines in phylogenetic analyses.

The specimens from the Lunan Basin that were referred to as *Forstercooperia* sp. (PGM V799, PGM V806, and PGM V 07, probably from one individual) are slightly larger than *P. confluens* in size (Chow et al., 1974). The complete M3 (PGM V799) resembles that of *P. confluens*, but differs from that of *Forstercooperia* by having a trace of metacone, straight protoloph, short ectoloph, and well-developed lingual cingulum. In addition, the fragmentary mandibles (PGMV 806, PGM V807) have a shallow mandibular ramus (Chow et al., 1974), which is also similar to that of *P. confluens* and distinguished from *F. ulanshirehensis*. These specimens are likely referable to *P. confluens*.

A cranial fragment with complete cheek teeth and canine alveoli (IVPP V5075) was assigned to *Pappaceras* sp. (Wang, 1976). This specimen is typically characteristic of forstercooperiines in having large upper canines (represented by large alveoli), and transversely wide outlines of upper premolars. Despite its larger size (length of M1–3 ~105.5 mm), it uniquely resembles *P. confluens* in sharing a trapezoidal outline of M3 with a distinct trace of metacone. There seems no doubt that this specimen has an affinity with *Pappaceras*, probably *P. confluens*, but the hypothesis that variation in body size is related to sexual dimorphism in *Pappaceras* requires further testing.

Zhai (1977) assigned a fragmentary maxilla with M1–3 and some isolated check teeth (IVPP V5241) to *Forstercooperia* sp. ("*Imequincisoria* sp."), this assignment appears inappropriate as suggested by Qiu and Wang (2007), because it is distinct from forstercooperiines with the hypocone of P2 lingually positioned, the metaloph of P3 posteriorly extended, the ectoloph of M1–2 straight, and the well-developed entoconid of p4. Meanwhile, the evidence for the age of the Changxindian Formation is apparently contradictory based on the records of fossil mammals, fossil invertebrates, and plants (including gastropods and pollens) in Zhai's proposal. These rhinocerotoid specimens might belong to later derived rhinocerotoids (possibly late Eocene taxa) rather than forstercooperiines.

Ding et al. (1977) referred a complete p3 (IVPP V5108.1) and p4 (IVPP V5108), and incomplete left m1–2 (IVPP V5109) as *Forstercooperia* sp. The tooth crown of IVPP V5109 is badly damaged and less characteristic for detailed comparisons. The p3 and p4 (IVPP V5108.1 and V5108) are at least 20% larger than those of *F. ulanshirehensis* (IVPP V20155 and V20156), furthermore they have well-developed entoconids and entolophids, which are rarely present in *Forstercooperia*. Therefore, the two specimens are unlikely to belong to *Forstercooperia*, and might be referable to paraceratheriines.

Comparisons with Other Early Rhinocerotoids

Forstercooperia is one of the most poorly known rhinocerotoid genera due to its poor preservation. Previously, forstercooperiines were usually assigned to the broad hyracodontid group together with paraceratheriines, mainly considering the divergence of anterior dentition within rhinocerotoids (Radinsky, 1967; Prothero et al., 1986). In the latest study, the craniodental morphology of *Pappaceras* has been briefly compared with representatives of other early rhinocerotoids (Wang et al., 2016), Here comparisons between forstercooperiines and other early rhinocerotoids are further expanded by adding complete craniodental morphology of *Forstercooperia*, which also lays the grounds for improved exploration of the phylogeny of early rhinocerotoids.

Hyrachyus is commonly considered as ancestral or sister taxon to rhinocerotoids, though its taxonomy is in need of revision (Wang et al., 2016; Bai et al., 2017). Generally, forstercooperiines share several primitive features with *Hyrachyus* that are characteristic of primitive tapiromorphs, such as a dolichocephalic cranium structure, long nasal, shallow narial notch, premaxilla-nasal contact, slender zygomatic, complete dentition (except for *P. meiomenus*), and primitive premolars. However, the new specimens of *F. ulanshirehensis* demonstrate there remains a distinct morphological gap between *Hyrachyus* and *Forstercooperia*. *Hyrachyus* lacks a distinctive preorbital fossa, which is shallow in *Forstercooperia*. The distance between the postglenoid process and the occipital condyle is short in *Hyrachyus* (*Hyrachyus eximius*) (13% of the skull length) (Wood, 1934), whereas it is much longer in *Forstercooperia* (AMNH 21608) (>25% of the skull length). Similar to most primitive tapiromorphs and different from forstercooperiines, the posttympanic process of *Hyrachyus* is considerably shorter than the paroccipital process, which is slender, oriented slightly posteriorly, and completely separated from the posttympanic process. *Forstercooperia* differs from *Hyrachyus* in several derived dental features: well-developed transverse lophs of cheek teeth, small parastyles of cheek teeth, slightly separate protocone and hypocone of P2, clearly reduced metacone and metastyle of M3, relatively elongated talonids of p2–4, and the presence of an entoconid in p4. The similarity of cranial morphology between *Forstercooperia* and *Hyrachyus* is indicative of the primitive status of the former, but the craniodental differences between them reveal that *Forstercooperia* is an unequivocal rhinocerotoid, more derived than *Pappaceras*, with several aforementioned derived dental features, such as triangular M3, which are shared by most of the later rhinocerotoids.

Triplopus is regarded as the most primitive and typical hyracodontid with its earliest record in Early Uintan (NALMA) North America (Prothero, 1998; Prothero et al., 1986). It is contemporary with *Forstercooperia* (*F. totadentata* and *F. ulanshirehensis*). *Triplopus cubitalis*, which was erected, described, and measured based on an incomplete skeleton (AMNH 5095) by Cope (1884), is considerably smaller than *Forstercooperia* (with the length of the skull ~128 mm). The facial region of *T. cubitalis* is distinctly shorter than that of *Forstercooperia*, with the anterior border of orbital situated at about one-third of the cranial length (though its incompleteness of the anterior tip). Compared with *Forstercooperia*, *T. cubitalis* has a much broader frontal that distinctively overlaps the orbital region with a ratio of the zygomatic width to the skull length about 1:2 (zygomatic width 64 mm, length of skull 128 mm in AMNH 5095), whereas the ratio is probably less than 40% in *Forstercooperia* (zygomatic width slightly more than 182

mm, cranial length more than 455 mm in AMNH 21608). The glenoid fossa is broad both in *Triplopus* and *Forstercooperia*, but the postglenoid process of the latter is more massive than that of the former. The postglenoid process is further separated posteriorly from the posttympanic process in *Triplopus*, forming a large external meatus, while in *Forstercooperia* the posttympanic process is ventrally expanded to be close to the postglenoid process. In addition, the posttympanic process and paroccipital process are slender and separated from each other in *T. cubitalis*, while these two processes are partially fused in *Forstercooperia*. The sagittal crest of *T. cubitalis*, as well as the weak parietal crest, is less developed than that of *Forstercooperia*, which is comparatively high and strong. The anterior dentition of *T. cubitalis* remains primitive, comprised of spatulate incisors and slender canines, which are different from the conical specialization of upper incisors and stubby canines of *Forstercooperia*. *T. cubitalis* shares several features with *Forstercooperia* in the upper cheek teeth, such as primitive upper premolars, distinct paracone and metacone ribs of upper premolars, and a elongated metastyle of M2. They are easily distinguished from each other by following aspects: (1) the metalophs (metaconules) of upper premolars are more developed in *T. cubitalis* than in *Forstercooperia*; (2) the protolophs of upper premolars are more curved to contact the metaconules in *T. cubitalis*, nearly forming a lingual loop, than the straight form of *Forstercooperia*; (3) the premolars of *T. cubitalis* are nonmolarized, but the P2s display the rudimentary distinction of protocone and hypocone and the p4s have entoconids in *Forstercooperia*; (3) the parastyle is relatively larger and located far from the paracone in the cheek teeth of *T. cubitalis*, while *Forstercooperia* has smaller parastyles on the upper cheek teeth, which are closely situated with the paracone. The molars of *T. cubitalis* usually are distinguished from derived hyracodontids by their lack of ornaments, such as crochet and antecrochet, whereas an antecrochet is present in the M1 of *Forstercooperia*. The M3 of *T. cubitalis* differs from that of *Forstercooperia* with a distinct metacone and metastyle. Despite the contemporaneity of *T. cubitalis* and *Forstercooperia* (both *F. totadentata* and *F. ulanshirehensis*), the craniodental difference between *Triplopus* and *Forstercooperia* reflects the distinct morphological gap between hyracodontids and forstercooperiines, suggesting that these two groups are unlikely to be closely related.

Hyracodon is a derived hyracodontid from North America (Radinsky, 1967) that also shares several primitive craniodental features with *Forstercooperia*, such as the large premaxilla with a distinct ascending branch, large facial exposure of the lacrimal, well-developed sagittal crest, and complete dentition. Compared with well-preserved crania of *Hyracodon* (*H. nebraskensis*) (AMNH 12296, 12460), *Forstercooperia* (length of cranium over 455 mm) is considerably larger than *Hyracodon* (length of cranium ~290 mm). The nasal of *Forstercooperia* bears a thin profile in cross section, whereas *Hyracodon* shows the derived condition of reduced nasals with a triangular cross section that medially contact and curve slightly, forming a distinct groove along the suture. The facial region, relative to the skull length, is longer in *Forstercooperia* than in *Hyracodon*. The reason is that the maxilla of *Forstercooperia* is more anteroposteriorly extended than that of *Hyracodon*. Particularly, the anterior border of the orbit is situated almost at the middle point of the cranium (the boundary of M2/3) in *Forstercooperia*, while it is much more anteriorly located (the boundary of M1/2) in *Hyracodon*. The lacri-

mal tubercle is rather weak and the lacrimal fossa is more medially situated in *Forstercooperia*, while there is a well-developed lacrimal tubercle and two distinct lacrimal fossae on the posteroventral border of the orbit in *Hyracodon*. The ventral surface of the palatines in *Forstercooperia* is nearly flat (or slightly concave), and probably possesses a pair of incisive foramina (assumedly similar to *Pappaceras*). This is distinguished from that of *Hyracodon*, in which a single incisive foramen is present, and a distinctive crest rises posteriorly at the level of P2 along the suture of the palatines. This crest appears to be unique to *Hyracodon* among all early rhinocerotoid groups. The pterygoid fossa is rather weak in *Forstercooperia*, *Pappaceras*, and most primitive rhinocerotoids, but it is clearly well developed in *Hyracodon*. Similar to *Triplopus*, *Hyracodon* lacks the unique characteristics of the basicranium in *Forstercooperia* and *Pappaceras*. The postglenoid foramen is present in *Hyracodon*, but absent in *Forstercooperia*. The anterior surface of the postglenoid process lacks ridges in *Hyracodon* and other typical hyracodontids, and this is different from forstercooperiines, amynodontids, and rhinocerotids, in which it is divided into two surfaces by a median ridge (Wang et al., 2017). Correspondingly, the postcotyloid process of the mandibles is absent in hyracodontids, but present in other rhinocerotoids despite the variation of shape and orientation (Wang et al., 2017). In particular, the postcotyloid process is characteristic of rhinocerotids, but clearly weak in paraceratheriids and amynodontids. The short posttympanic process of *Hyracodon* has a sharp lateral margin, and is posteriorly separated from the paroccipital process by a distinctive groove without the posttympanic-paroccipital foramen in lateral view. This is not the case in *Forstercooperia*, for which the posttympanic process is ventrally thickened and partially fused with the paroccipital process and the posttympanic-paroccipital foramen is present. The mandibular symphysis of *Hyracodon* is transversely more constricted in width than that of *Forstercooperia*. The posterior border of the ascending ramus in *Hyracodon* is more anteriorly inclined than in *Forstercooperia*.

Forstercooperia is also clearly distinguishable from *Hyracodon* by a number of dental characteristics. Despite the similarity of their generally conical incisors, *Forstercooperia* has subequal and stubby incisors (I2 slightly larger than I1 and I3), while all incisors of *Hyracodon* are distinctively slender and conical (I1/i1 slightly larger than other incisors) accompanied by a reduced mandibular symphysis. The upper canine of *Forstercooperia* is much stubbier and larger than the incisors, similar to that of amynodontids and eggysodontids. This is different from the upper canine of *Hyracodon*, which has a slender, conical, and incisorlike outline. *Forstercooperia* possesses primitive upper premolars, of which only P2 has barely separate protocone and hypocone, whereas the upper premolars of *Hyracodon* show a higher molarization and the hypocone and metaloph are well developed. The ribs of the protoloph and metaloph on the buccal wall are distinct in *Forstercooperia*, but weak in *Hyracodon*. The antecrochets of M1–2 are weak in *Forstercooperia*, whereas they are well developed in *Hyracodon*. The metastyle of M2 is elongated and lingually extended in *Forstercooperia*, while relatively straight in *Hyracodon*. The M3 of *Forstercooperia* lacks the metastyle, unlike that of *Hyracodon*, in which there remains a short but evident metastyle on the posterior side of the ecto-metaloph. The derived features of the lower cheek teeth of *Hyracodon* are consistent with the upper. The p1

is reduced in *Hyracodon*, different from all forstercooperiines except for *Pappaceras meiomenus*. Also, the lower premolars of *Hyracodon* are distinctly molarized with well-developed entoconids and entolophids. In contrast to *Hyracodon*, all lower premolars of forstercooperiines remain primitive without the entolophid, and the entoconid in the lower premolars only appears in the p4 of *F. ulanshirehensis*.

Another subgroup of derived hyracodontids is represented by the Asian *Ardynia* (*A. praecox* and *A. kazachstanensis*) (Matthew and Granger, 1923; Beliajeva, 1952; Radinsky, 1967). *Forstercooperia* is similar to *Ardynia* (AMNH 26039 and AMNH 26183) in several features: premaxilla-nasal contact, slender zygomatic arch, and complete anterior dentition. Similar to other hyracodontids, *Ardynia praecox* differs from *Forstercooperia* in several aspects. Compared with conical and equal-sized upper incisors of *Forstercooperia*, *Ardynia* retains the primitive spatulate, loosely spaced upper incisors, of which I1 is larger than I2 and I3. Similar to other hyracodontids, the upper canine of *Ardynia* is reduced and smaller than the upper incisors, unlike the stubby canines of forstercooperiines. *Ardynia* also exhibits the reduction of premolars by the absence of P1/p1 and the presence of single-rooted p2s, whereas within forstercooperiines the reduction of P1/p1 is present only in *P. meiomenus*. On the other hand, the diastema between canines and cheek teeth is longer in *Ardynia* than that in *Forstercooperia*. The upper premolars of *Ardynia* are derived with distinct protolophs and metalophs, whereas *Forstercooperia* possesses weak metalophs or metaconules only in the upper premolars. Differing from *Hyracodon*, the M3 of *Ardynia* is more derived than *Forstercooperia* and early hyracodontids by the absence of metacone and metastyle, and the presence of the convex posterior wall of ecto-metaloph. The lower cheek teeth of *Ardynia* are distinguished from those of *Forstercooperia* and most other rhinocerotoids by a uniquely V-shaped trigonid, resulting from a short paralophid and considerably lingually directed protolophid. In addition, *Ardynia* bears a ridge on the ventral surface of the palatines, which is probably unique for derived hyracodontids (like *Hyracodon*). Although the ascending part of the premaxilla in *Ardynia* is relatively extensive, the narial notch is more posteriorly located at the level of P2, deeper than those of forstercooperiines. The paroccipital process of *Ardynia* is considerably more slender and narrower than those of forstercooperiines. The mandibular symphysis of *Ardynia* is relatively elongated and more anteriorly extended (rather than constricted as in forstercooperiines), and similar to those of most primitive tapiromorphs.

Rostriamynodon grangeri (AMNH 107635) is the earliest representative of amynodontids with an age of Arshantan (Wall and Manning, 1986). It is another rhinocerotoid genus contemporary with *Forstercooperia* (*F. totadentata* and *F. ulanshirehensis*). *Rostriamynodon* also shares a few primitive features with *Forstercooperia*, including premaxilla-nasal contact, nasal-lacrimal contact, a distinct preorbital fossa, and a slightly concave ventral surface of the palatines and large canines. However, *Forstercooperia* obviously differs from *Rostriamynodon* in numerous craniodental features. The skull of *F. ulanshirehensis* is smaller than that of *Rostriamynodon*; the latter is about 560 mm in length and presumably close to that of *F. totadentata* (Wall and Manning, 1986). The anterior tip of the nasal in *Forstercooperia* is slightly narrower, similar to that of *Hyrachyus* or *Triplopus*, whereas it is generally rounded in *Rostriamynodon*

and close to other amynodontids (like *Amynodon*) and derived rhinocerotids. The preorbital fossa of *Forstercooperia* is slightly shallower than that of *Rostriamynodon* and later amynodontids. The lower incisors of *Forstercooperia* are larger and more conical than those of *Rostriamynodon*, which are primitively spatulate, tightly spaced between lower canines, and relatively small. The lower canine of *Forstercooperia* is stubby but not tusklike, whereas *Rostriamynodon* bears more tusklike lower canines with sharp mesial and distal ridges. There remains a complete premolar series in *Forstercooperia* (neither the reduction of P1/p1, nor is there the anteroposterior constriction of the premolar series), whereas *Rostriamynodon* shows the absence of the first premolar and shortened premolar series, which are characteristic of amynodontids (like *Amynodon*) and derived hyracondontids (like *Triplopides* and *Ardynia*). The diastema of *Forstercooperia* is slightly shorter than *Rostriamynodon*. In addition, the upper cheek teeth of *Forstercooperia* are less quadrate in outline than those of *Rostriamynodon*, despite the poor preservation of the upper molars of *Rostriamynodon*. Specifically, the M3 of *Forstercooperia* has a triangular outline, distinct from the quadrate form of *Rostriamynodon*, which is attributed to the completeness of the metacone and ectoloph of M3. Also, the upper premolars of *Forstercooperia*, especially P4, are slightly transversely narrower than those of *Rostriamynodon*, and this is reflected by the ratio of width to length of P4, which is less than 1.5 in *Forstercooperia* (~1.3 for *F. ulanshirehensis*), but more than 1.5 in *Rostriamynodon*. Corresponding to the upper cheek teeth, the lower cheek teeth of *Rostriamynodon* also display characteristics of amynodontids; for instance, the metalophids of lower molars are considerably extended anterolaterally rather than laterally as in non-amynodontid rhinocerotoids. In addition, the mandibular angle of *Forstercooperia* is more rounded than that of *Rostriamynodon*.

The new occurrence of *Forstercooperia* is definitely significant for comprehensive comparative study of paraceratheriids (paraceratheriines and forstercooperiines) after Qiu and Wang's work in 2007, further narrowing the morphological gap between forstercooperiines and paraceratheriines. *Juxia sharamurenensis* (IVPP V2891) is widely regarded as the direct ancestor or sister taxon of later giant rhinos, and it occurs in the Sharamurun Formation and the "Ulan Gochu Formation" of the Shara Murun and Urtyn Obo areas, Nei Mongol, China, which is commonly regarded as stratigraphically younger than the Irdin Manha Formation (Chow and Chiu, 1964; Qiu and Wang, 2007). Qiu and Wang (2007) proposed that paraceratheriids possess an elongated posterior cranial portion, which is reflected by the percentage of the length from the postglenoid process to the condyle to the length from P1 (or P2) to the condyle. It is greater than or equal to 25% for *Juxia* and later paraceratheriids, which is partially attributed to the enlargement of the posttympanic process, paroccipital process, and occipital condyle. Forstercooperiines have a similar ratio to paraceratheriids, about 0.22 for *P. meiomenus* (IVPP V 20254) (Wang et al., 2016), and 0.26 for *F. ulanshirehensis* (AMNH 21608) (table 1). The nasal-premaxilla contact is primitively present in *Forstercooperia*, but already lost in *J. sharamurenensis*. The narial notch of *Forstercooperia* is shallow with its posterior margin at the upper canine level, whereas in *J. sharamurenensis* it is more posteriorly located above P2. The anterior border of the orbit is more posteriorly located above the anterior end of M3 in *Forstercooperia* than it is in *J. sharamurenensis*, on which it is situated above the anterior end of M2. Further-

more, the new specimens of *Forstercooperia* reveal that morphological gaps still remain between *Forstercooperia* and *Juxia* in the basicranium. Compared with other early rhinocerotoids, the posttympanic process of *Forstercooperia* is clearly anteroposteriorly thickened, similar but still rudimentary compared to that of *Juxia*. The posttympanic process and paroccipital process have different heights, relatively slender outlines (especially the paroccipital process), and are closely situated but incompletely fused in *F. ulanshirehensis*, whereas they are roughly equal in height, nearly vertically situated, and completely fused with a transversely blunt outline in *J. sharamurenensis*. The ratio of the height of the occipital condyle to its width is about 1.2 in both *F. ulanshirehensis* and *J. sharamurenensis* (table 1), but the size of the occipital condyle in the former is smaller than that in the former (height:width: 42.96:35.95 mm vs. 60:50 mm). Otherwise, *Juxia* is the earliest record of distinct enlargement of I1/i1 and procumbent i1, which are regarded as significant characteristics of Paraceratheriinae (Lucas and Sobus, 1989; Qiu and Wang, 1999, 2007). *Forstercooperia* is easily distinguished from *Juxia* by the absence of unique specialization of I1/i1. Additionally, the stubby canines in *Forstercooperia* are also different from the incisorlike canines of *Juxia*. The earlier stratigraphic occurrence of *Forstercooperia* relative to *Juxia* seems consistent with the morphological distinction of upper premolars between the two genera. Specifically, *Forstercooperia* possesses more primitive premolars than *Juxia*, showing that the separation of protocone and hypocone is present only in P2 of *Forstercooperia*, but that separation occurs in P2–3 of *J. shramurenensis* along with the presence of well-developed metaloph of P2. Meanwhile, the protolophs of P3–4 are transversely straight in *Forstercooperia*, but more posteriorly extended at the lingual side in *J. shramurenensis*. Similarly, among lower premolars, the entoconid is present in p3–4 of *J. shramurenensis*, whereas only p4 has a weak entoconid in *F. ulanshirehensis*.

Teletaceras is considered the most primitive rhinocerotid (Hanson, 1989; Prothero, 2005). It displays craniodental features that are generally shared by primitive tapiromorphs (including forstercooperiines), such as a small to medium size, dolichocephalic structure, complete dentition, and primitive premolars. In addition, *Forstercooperia* has derived features that are characteristic of rhinocerotids, such as a medial ridge on the ventral surface of the glenoid fossa, a weak postcotyloid process, and a distinct median crest on the ventral surface of basioccipital. However, *Forstercooperia* is clearly distinguished from *Teletaceras* in the following aspects: (1) the nasal is transversely wider and relatively thinner than that of *Teletaceras*, which has a triangular cross section and tapers gently; (2) the narial notch is above the upper canine and shallower than that of *Teletaceras*, which is above the postcanine diastema; (3) the frontal is much wider than in *Teletaceras*; (4) the facial region is more elongated with the anterior border of orbital above the boundary of M2–3, rather than above the boundary of M1–2 as in *Teletaceras*; (5) the sagittal crest is relatively high and distinct, more developed than that of *Teletaceras*, in which the supratemporal crests converge at the midline to form a low and narrow sagittal crest; (6) the postglenoid foramen is absent in *Forstercooperia*, but present in *Teletaceras*; and (7) the posttympanic process is thickened and partially fused with and the paroccipital in *Forstercooperia*, while the two processes are considerably slender and completely separated in *Teletaceras*. Meanwhile, the differences in dental characters between *Forstercooperia* and

Teletaceras demonstrate that they are not closely related. The most diagnostic character of *Teletaceras* lies in the anterior dentition. Despite the incompleteness of the anterior dentition, *Teletaceras* (UCMP 129009) differs from *Forstercooperia* with distinctively enlarged and tusk-like I1 and i2, which are the earliest records of the diagnostic rhinocerotid features. The I1 of *Teletaceras* has a single wear facet compatible with the i2, whereas the I1 in forstercooperiines has two wear facets compatible with lower incisors (i1 and i2). According to the original reconstruction (Hanson, 1989: fig. 20), the I1 and i2 are probably larger than other incisors, as in other rhinocerotids. This is distinct from the conical and subequal incisors of *Forstercooperia*. The canines are reduced in size and conical in *Teletaceras*, but rather stubby and large in *Forstercooperia*. The protolophs of upper premolars that are posteriorly extended at lingual side in *Teletaceras* differ from those of *Forstercooperia*. The metaconules of P3–4 are extended more posterolingually in *Teletaceras*, whereas they are relatively transversely straight in *Forstercooperia*. The M3 of *Teletaceras* still retains a small trace of metacone and metastyle, but *Forstercooperia* lacks the metacone and metastyle of M3, possessing a distinctly triangular outline.

Eggysodontids are one of the most poorly known rhinocerotoid groups and include four genera to date: *Proeggysodon* Bai and Wang, 2012; *Guangnanodon* Wang et al., 2013; *Eggysodon* Roman, 1911; and *Allacerops* Wood, 1932. The former two are represented by fragmentary mandibles from the Upper Eocene of northern China. The earliest-known eggysodontid, *Proeggysodon*, shows some similarity to *Pappaceras confluens* in its smaller size, short diastema, and large lower canines (Bai and Wang, 2012). Compared with *Forstercooperia*, the Eocene genus *Proeggysodon* is distinguished by its smaller size, broad mandibular symphysis (rather than transversely narrow or constricted as in forstercooperiines), primitively spatulate lower incisors, and reduction of lower incisor number. *Guangnanodon* differs from *Forstercooperia* in the presence of entoconids and weak entolophids of p3–4 and the short paralophids of the lower molars (Wang et al., 2013). The Oligocene eggysodontids *Eggysodon* and *Allacerops* are, despite their relatively large size (length of m1–3 ~80–96.7 mm), still smaller than those of *Forstercooperia* (Radinsky, 1967; Reshetov et al., 1993; Qiu and Wang, 1999; Uhlig, 1999; Bai and Wang, 2012; Wang et al., 2013). Although the Oligocene eggysodontids show some variation in the number of incisors (2 or 3) and premolars (3 or 4), they are distinct from *Forstercooperia*, with more molarized upper and lower premolars, of which P3–4 have fully separated hypocones and strong metalophs, and their p3–4s have well-developed entoconids and entolophids (Reshetov et al., 1993; Qiu and Wang, 1999; Uhlig, 1999). Based on the recently reported fragmentary cranium of *Eggysodon*, Antoine et al. (2011) have listed a few apomorphic traits of eggysodontids, for instance, a short nasal and weak posttympanic and paroccipital processes, which are considerably distinct from those of forstercooperiines and roughly similar to rhinocerotids. Compared with *Forstercooperia*, the mandibular symphysis of *Eggysodon* is more upright and the posterior margin of the ascending ramus is distinctively inclined forward. Although eggysodontids are not comprehensively known from the current collection, the evidence is indicative of a morphological gap between forstercooperiines and eggysodontids.

Holbrook and Lucas (1997) established *Uintaceras* to encompass most of the North American "forstercooperiines" that were formerly assigned to *Forstercooperia* by Radinsky

(1967) and Lucas et al. (1981) and proposed a novel affinity between *Uintaceras* and rhinocerotids. This genus is somewhat unique within rhinocerotoids mainly because of its anterior dentition. In the phylogenetic results suggested by Holbrook and Lucas (1997), the *Uintaceras*-rhinocerotid clade is moderately supported by the synapomorphy of the buccolingually compressed upper incisors. This feature seems uniquely distinctive across all rhinocerotoids, given the morphological gap of anterior dentition between *Uintaceras* and *Teletaceras*, the earliest representative of rhinocerotids. The similarities of postcranial features between *Uintaceras* and amynodontids and rhinocerotids were also already discussed (Holbrook and Lucas, 1997), including the rhomboidal radial facet of the scaphoid, the distal process of the posterior ectocuneiform, the prominent, laterally hooking deltopectoral crest, and robust, noncursorial limbs; these are as significant as the features of the anterior dentition, although this resemblance was regarded as a scaling deviation in their paper. Furthermore, the similarities among *Uintaceras*, forstercooperiines (*Pappaceras*), and amynodontids have been broadly discussed (Wang et al., 2016), supporting a close affinity among these three groups. More importantly, the new specimens of *F. ulanshirehensis* reinforce the similarity between forstercooperiines and *Uintaceras*, demonstrating the close relationship between *Uintaceras*, amynodontids, and paraceratheriids. The postglenoid process of *Uintaceras* is massive and transversely broad, similar to forstercooperiines. The posttympanic and paroccipital processes in *Uintaceras*, which are relatively enlarged and extended ventrally rather than posteroventrally, are most comparable to those of paraceratheriids within early rhinocerotoids. The diagnostic posttympanic-paroccipital foramen is present both in *Uintaceras* and paraceratheriids. The resemblance of dental features between *Uintaceras* and forstercooperiines has been discussed by several authors (Radinsky, 1967; Lucas et al., 1981; Holbrook and Lucas, 1997), and the cheek teeth of *Uintaceras* are most comparable to those of forstercooperiines with the presence of strong ribs on upper premolars, protolophs of upper premolars posteriorly extended (similar to *Pappaceras confluens*), antecrochet of M1–2, and relatively distinct metacone and short metastyle of M3 (similar to *Pappaceras minuta* and *Pappaceras meiomenus*). On the other hand, *Uintaceras* can be distinguished from forstercooperiines by its narial incision deeper above P1 and the anterior border of orbital located above M1–2 (Holbrook and Lucas, 1997). Consequently, we conclude that *Uintaceras* has uniquely mosaic features of early rhinocerotoids, suggesting that this former "forstercooperiine" genus should be closer to forstercooperiines rather than to rhinocerotids.

Phylogenetic Analysis

Only one most-parsimonious tree is returned from the phylogenetic analysis as below (fig. 10). Similar to the recent study by Wang et al. (2016), the primary groups of early rhinocerotoids (Hyracodontidae, Amynodontidae, Paraceratheriidae, Eggysodontidae, and Rhinocerotidae) are monophyletic. The monophyly of hyracodontids is well supported from the results of the phylogenetic analysis, showing relatively high Bremer support values for the nodes within the hyracodontid clade, despite the exclusion of some taxa con-

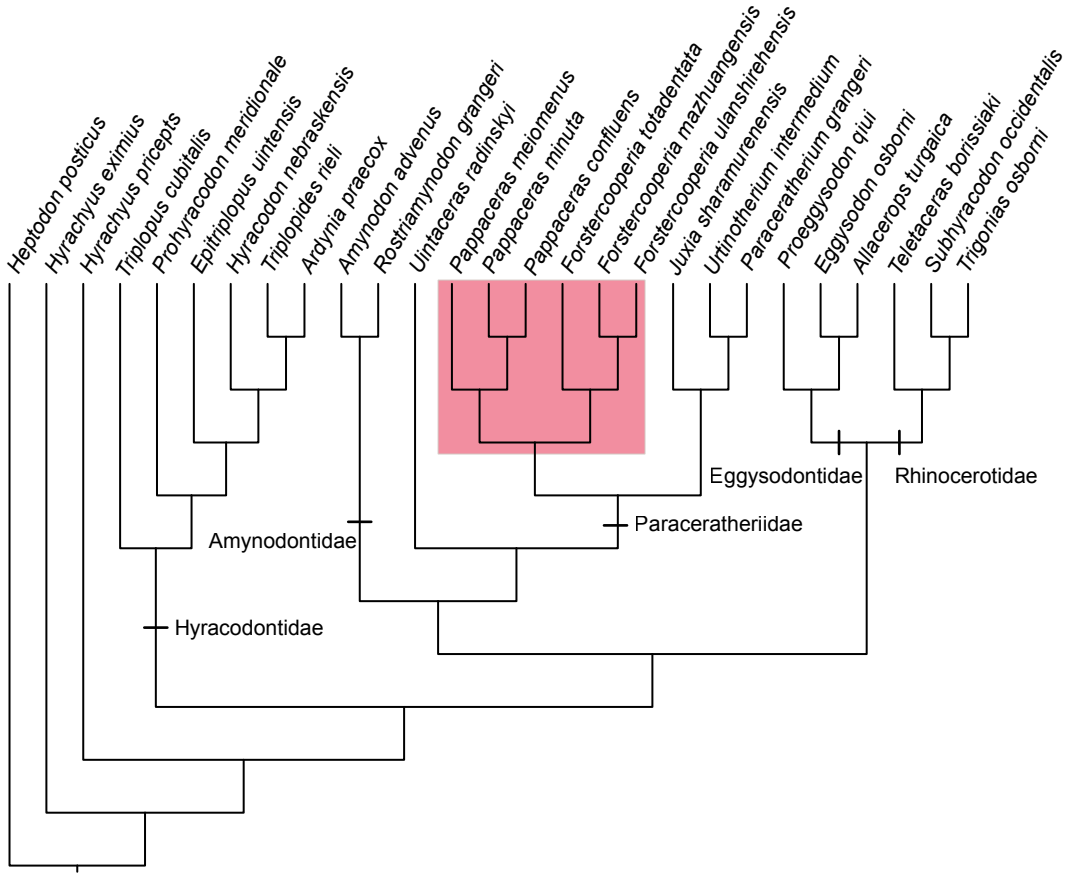

FIG. 10. Phylogenetic relationships of early rhinocerotoids based on the single most-parsimonious tree returned from phylogenetic analyses. The number by each node denotes the Bremer Support value. Tree length = 433, CI = 0.536, RI = 0.714. The forstercooperiine clade is marked by the pink rectangle.

ventionally included in the hyracodontids (e.g., Radinsky, 1967; Prothero et al., 1986; Wang et al., 2016). The amynodontid clade is the most stable group in the phylogenetic analysis with a high Bremer support value. This clade is closely related to the paraceratheriids and *Uintaceras*, but the monophyly of these three clades is moderately supported due to character conflicts. For instance, the dentition of amynodontids exhibit numerous unique features distinct from those of other rhinocerotoids. After adding *F. ulanshirehensis* and *F. mazhuangensis* to the data matrix, the phylogeny of the monophyletic forstercooperiine clade has better resolution than the previous study (e.g., Wang et al., 2016), demonstrating the monophyly of *Pappaceras* and *Forstercooperia* in a phylogenetic context for the first time. This is in contrast to the previous argument that all species of forstercooperiines were congeneric (*Forstercooperia*) (e.g., Radinsky, 1967; Lucas et al., 1981). Contrary to the latest study (Wang et al., 2016), the interrelationship of three species of *Pappaceras* is well resolved, showing that *P. confluens* and *P. minuta* are closer to each other than to the newly erected species *P. meiomenus*. However, the new species *F. ulanshirehen-*

sis is clustered with *F. totadentata* and *F. mazhuangensis*, and the interrelationships of these three species of *Forstercooperia* are unresolved. This result is not unexpected because *F. totadentata* and *F. mazhuangensis* are represented only by fragmentary crania and incomplete dentition, and as such the character matrix lacks many character-state codings for the two species. Furthermore, the monophyletic clade comprising paraceratheriids and *Uintaceras* is moderately supported, which is probably attributed to conflicting phylogenetic signals from a sizable part of autapomorphies of *Uintaceras* (Holbrook and Lucas, 1997; Wang et al., 2016). The enigmatic eggysodontid clade, which comprises three genera represented by incomplete fossils, is placed as the sister group of rhinocerotids. This novel result is in contrast to the previous views regarding either hyracodontid or paracerotheriid affinity for eggysodontids (Radinsky, 1967; Reshetov et al., 1993; Qiu and Wang, 1999; Uhlig, 1999; Bai and Wang, 2012; Wang et al., 2013). However, this question is in need of further investigation based on more morphological data added to the present character matrix, in particular, from more complete Eocene specimens.

Biostratigraphic Implication

Generally, stratigraphic correlations are the basis for the correlative relationships of biostratigraphic units or zones within particular areas. The Paleogene stratigraphic framework of the Erlian Basin has already been established based on numerous investigations since the 1890s as summarized by Wang et al. (2012) and Meng et al. (2007), such that four faunas (Arshantan, Irdinmahan, Sharamurunian, Ulangochuan) from this area have laid the ground for the Paleogene Asian Land Mammal Ages in the geologic time scale (Gradstein et al., 2012). But there still remains some confusion regarding fossil locality names and lithostratigraphic units, some of which have been discussed and corrected in a recent study after detailed field investigation over the last decade (Wang et al., 2012). The correction of fossil locality names and lithostratigraphic correlations inevitably affects biostratigraphic correlations. In terms of the locality names involved in the present study, the localities from which the new specimens (AMNH 21608 and 22101) were collected were originally described as "8 miles north of Tukhum Lamasery" and "4 miles north of Tukhum Lamasery," respectively (Granger, 1925, 1928). Based on the detailed fieldwork and comprehensive comparisons by an international team composed of staff from IVPP, AMNH, and CMNH (Meng et al., 2007; Wang et al., 2010, 2012), the two localities should be regarded as the Wulanhuxiu site and Wulantaolegai site of the western part of Erlian Basin respectively. With regard to the lithostratigraphic units, the mentioned specimens (AMNH 21608 and 22101) were unearthed from the Ulan Shireh Formation, although the correlation between the sediments and the eastern part of the Erlian Basin is still unclear. Conventionally, the Ulan Shireh Formation was correlated to the Irdin Manha Formation (Granger and Gregory, 1934; Granger, 1938; Ye, 1983; Wang et al., 2012), but recent investigation demonstrates that the mammalian fauna from the Ulan Shireh Formation is probably composed of both Arshantan and Irdinmanhan taxa (Wang et al., 2012). The latest study of the mammal fauna from the Ulan Shireh Forma-

tion at the Wulanhuxiu site provided a detailed description of the recently discovered small mammals, summarized the mammal records from this area, and discussed faunal turnover in the Chinese Eocene record (Li et al., 2016). That work suggests that the faunal assemblage is much more complex than previously thought, proposing that the lower fossiliferous bed (horizon 4) is indicative of an Irdinmanhan age chiefly with a typical assemblage of perissodactyls (Li et al., 2016: table 1), while the upper horizon (horizon 2) is probably Sharamurunian (or post-Irdinmanhan) in age with abundant remains of Sharamurunian *Gobiolagus* (Meng et al., 2005; Li et al., 2016). Combining the field notes recorded by Granger and recent investigations, the lower part of the Ulan Shireh Formation (e.g., horizon 4 at the Wulanhuxiu site, see Li et al., 2016) yields a considerable number of fossils (mainly dominated by perissodactyls and Glires), whereas the upper part, containing less abundant fossil material, may be equivalent to the Tukhum Formation, which is another lithostratigraphic unit in the western part of the Erlian Basin (Wang et al., 2012). The stratigraphic information for the two specimens in the collection database is extremely limited, and it is impossible to ensure which lithostratigraphic bed of the Ulan Shireh Formation contained them (AMNH 21608 and AMNH 22101). It is highly possible that the two specimens were unearthed from the lower part of the Ulan Shireh Formation, judging from the preservation condition (H.-B.W., personal obs.) and the dominant component of perissodactyls in this faunal assemblage. If this hypothesis is correct, their occurrence would lend support to the notion that the lower part of the Ulan Shireh Formation is equivalent to the Irdin Manha Formation in the eastern part of the Erlian Basin, where the other three specimens of *F. unlanshirehensis* (IVPP V20154, V20155, V20156) were recovered. In that case, forstercooperiines are Arshantan-Irdinmanhan in age, with the smaller, Arshantan-aged *Pappaceras* having a primitive dentition and the larger, Irdinmanhan-aged *Forstercooperia* having a derived craniodental morphology.

ACKNOWLEDGMENTS

We thank Zhan-Xiang Qiu, Zhao-Qun Zhang, Qian Li, Xun Jin, Fang-Yuan Mao, and Yan-Xin Gong (all IVPP) for discussion and assistance in the lab; Zhou Wei, Shi-Jie Li, Yong-Xing Wang, Yong-Fu Wang, and Qi Li (all IVPP) for assistance in fieldwork; Shi-Jie Li for specimen preparation; R. O'Leary, J. Galkin, and C. Mehling (all AMNH) for access to the specimens in their care; S. Bell (AMNH) for providing help with literature at AMNH. We are grateful to L. Holbrook (Rowan University) and M.C. Mihlbachler (New York Institute of Technology) for their critical and constructive suggestions, Z. Calamari, M. Knight, and R.S. Voss (all AMNH) for helpful suggestions with English and Yu Chen (IVPP) for the drawings. This work was supported by the National Science Foundation of China (grant no. 41572021 and 41672014), the Special Fund for Fossil Excavation and Preparation, CAS, State Key Laboratory of Palaeobiology and Stratigraphy (Nanjing Institute of Geology and Palaeontology, CAS) (grant no.163103), and the National Basic Research Program of China (grant no. 2012CB821904). Hai-Bing Wang was funded by the China Scholarship Council (CSC no. 201504910615).

REFERENCES

Antoine, P.-O. et al. 2011. A new late Early Oligocene vertebrate fauna from Moissac, south-west France. Comptes Rendus Palevol 10 (4): 239–250.

Bai, B., Y.Q. Wang, and J. Meng. 2010. New craniodental materials of *Litolophus gobiensis* (Perissodactyla, "Eomoropidae") from Inner Mongolia, China, and phylogenetic analyses of Eocene chalicotheres. American Museum Novitates 3688: 1–27.

Bai, B., and Y.Q. Wang. 2012. *Proeggysodon* gen. non., a primitive Eocene eggysodontine (Mammalia: Perissodactyla) from Erden Obo, Siziwangqi, Nei Mongol, China. Vertebrata PalAsiatica 50 (3): 204–218.

Bai, B., J. Meng, Y.Q. Wang, H.B. Wang, and L. Holbrook. 2017. Osteology of the middle Eocene ceratomorph *Hyrachyus modestus* (Mammalia: Perissodactyla). Bulletin of the American Museum of Natural History 413: 1–70.

Beliajeva, E.I. 1952. Primitivnye nosorogoobraznye mongolii. Akademia Nauk SSSR, Trudy Paleontologicheskogo Instituta 41: 120–143.

Chow, M.C., and C.S. Chiu. 1964. An Eocene giant rhinoceros. Vertebrata PalAsiatica 8 (3): 264–268.

Chow, M.C., Y.P. Zhang, and S.Y. Ting. 1974. Some early Tertiary Perissodactyla from Lunan Basin, E. Yunnan. Vertebrata PalAsiatica 12 (4): 262–273.

Cope, E.D. 1884. The vertebrata of the Tertiary formation of the West. Washington: Government Printing Office.

Ding, S.Y., J.J. Zheng, Y.P. Zhang, and Y.S. Tong. 1977. The age and characteristic of Liuniu and Dongjun faunas, Bose basin of Guangxi. Vertebrata PalAsiatica 15 (1): 35–45.

Gabounia, L. 1977. Contribution à la connaissance des mammifères paléogènes du Bassin de Zaïssan (Kazakhstan central). Geobios (Mémoire spécial 1): 29–37.

Goloboff, P.A. 1999. Analyzing large data sets in reasonable times: solutions for composite optima. Cladistics 15 (4): 415–428.

Goloboff, P.A., J.S. Farris, and K.C. Nixon. 2008. TNT, a free program for phylogenetic analysis. Cladistics 24 (5): 774–786.

Gradstein, F.M., J.G. Ogg, M.D. Schmitz, and G.M. Ogg. 2012. The geologic time scale 2012. Amsterdam: Elsevier.

[Granger, W.] 1925. [Records of fossils collected in Mongolia.] Field books of the Third Asiatic Expedition. American Museum of Natural History Library.

[Granger, W.] 1928. [Records of fossils collected in Mongolia.] Field books of the Third Asiatic Expedition. American Museum of Natural History Library.

Granger, W. 1938. A giant oxyaenid from the Upper Eocene of Mongolia. American Museum Novitates 969: 1–5.

Granger, W., and W.K. Gregory. 1934. An apparently new family of amblypod mammals from Mongolia. American Museum Novitates 720: 1–8.

Hanson, C.B. 1989. *Teletaceras radinskyi*, a new primitive rhinocerotid from the late Eocene Clarno Formation, Oregon. *In* D.R. Prothero and R.M. Schoch (editors), The evolution of perissodactyls: 379–398. New York: Oxford University Press.

Holbrook, L.T. 2001. Comparative osteology of early Tertiary tapiromorphs (Mammalia, Perissodactyla). Zoological Journal of the Linnean Society 132 (1): 1–54.

Holbrook, L.T., and S.G. Lucas. 1997. A new genus of rhinocerotoid from the Eocene of Utah and the status of North American "*Forstercooperia*." Journal of Vertebrate Paleontology 17 (2): 384–396.

Kretzoi, M. 1940. Alttertiare perissodactylen aus ungarn. Annales Historico-naturales Musei Nationalis Hungarici 33: 87–98.

Li, Q., Y.Q. Wang, and L. Fostowicz-Frelik. 2016. Small mammal fauna from Wulanhuxiu (Nei Mongol, China) implies the Irdinmanhan–Sharamurunian (Eocene) faunal turnover. Acta Palaeontologica Polonica 61 (4): 759–776.

Lucas, S.G., and J. Sobus. 1989. The systematics of indricotheres. *In* D.R. Prothero, and R.M. Schoch (editors), The evolution of perissodactyls: 358–378. New York: Oxford University Press.

Lucas, S.G., R.M. Schoch, and E. Manning. 1981. The systematics of *Forstercooperia*, a middle to late Eocene hyracodontid (Perissodactyla: Rhinocerotoidea) from Asia and western North America. Journal of Paleontology 55 (4): 826–841.

Matthew, W.D., and W. Granger. 1923. The fauna of the Ardyn Obo Formation. American Museum Novitates 98: 1–5.

Meng, J., Y.M. Hu, and C.K. Li. 2005. *Gobiolagus* (Lagomorpha, Mammalia) from Eocene Ula Usu, Inner Mongolia, and comments on Eocene lagomorphs of Asia. Palaeontologia Electronica 8 (1): 7A: 1–23.

Meng, J. et al. 2007. New stratigraphic data from the Erlian Basin: implications for the division, correlation, and definition of Paleogene lithological units in Nei Mongol (Inner Mongolia). American Museum Novitates 3570: 1–31.

Mihlbachler, M.C. 2008. Species taxonomy, phylogeny, and biogeography of the Brontotheriidae (Mammalia: Perissodactyla). Bulletin of the American Museum of Natural History 311: 1–475.

Nixon, K.C. 1999. The parsimony ratchet, a new method for rapid parsimony analysis. Cladistics 15 (4): 407–414.

Prothero, D.R. 1998. Hyracodontidae. *In* C.M. Janis, K.M. Scott, and L.L. Jacobs (editors), Evolution of Tertiary mammals of North America: Vol. 1, Terrestrial carnivores, ungulates, and ungulatelike mammals: 589–594. New York: Cambridge University Press.

Prothero, D.R. 2005. The evolution of North American rhinoceroses. Cambridge: Cambridge University Press.

Prothero, D.R., E. Manning, and B.C. Hanson. 1986. The phylogeny of the Rhinocerotoidea. Zoological Journal of the Linnean Society 87: 341–366.

Qi, T. 1987. The middle Eocene Arshanto fauna (Mammalia) of Inner Mongolia. Annals of the Carnegie Museum 56 (1): 1–73.

Qiu, Z.X., and B.Y. Wang. 1999. *Allacerops* (rhinocerotoidea, perissodactyla), its discovery in China and its systematic position. Vertebrata PalAsiatica 37 (1): 48–61.

Qiu, Z.X., and B.Y. Wang. 2007. Paracerathere fossils of China. Beijing: Science Press.

Radinsky, L.B. 1967. A review of the rhinocerotoid family Hyracodontidae (Perissodactyla). Bulletin of American Museum of Natural History 136 (1): 1–45.

Reshetov, V., N. Spassov, and B. Baishashov. 1993. *Tenisia* gen. nov.: taxonomic revaluation of the Asian Oligocene rhinocerotoid *Eggysodon turgacum* (Borissiak, 1915) (Mammalia, Perissodactyla, Hyracodontidae). Geobios 26 (6): 715–722.

Sahni, A. and S.K. Khare. 1973. Additional Eocene mammals from the Subathu Formation of Jammu and Kashmir. Journal of the Palaeontological Society of India 17: 31–49.

Uhlig, U. 1999. Die Rhinocerotoidea (Mammalia) aus der unteroligozänen Spaltenfüllung Möhren 13 bei Treuchtlingen in Bayern. Munich: Bayerische Akademie der Wissenschaften, Mathematisch-Naturwissenschaftliche Klasse, Abhandlungen 170.

Wall, W.P., and E. Manning. 1986. *Rostriamynodon grangeri* n. gen., n. sp. of amynodontid (Perissodactyla, Rhinocerotoidea) with comments on the phylogenetic history of Eocene Amynodontidae. Journal of Paleontology 60 (4): 911–919.

Wang, H.B., B. Bai, F. Gao, W.C. Huang, and Y.Q. Wang. 2013. New eggysodontid (Mammalian, Perissodactyla) material from the Paleogene of Guangnan Basin, Yunnan province, China. Vertebrata PalAsiatica 51 (4): 305–320.

Wang, H.B., B. Bai, J. Meng, and Y.Q. Wang. 2016. Earliest known unequivocal rhinocerotoid sheds new light on the origin of giant rhinos and phylogeny of early rhinocerotoids. Scientific Reports 6: 39607.

Wang, H.B., B. Bai, Y.X. Gong, J. Meng, and Y.Q. Wang. 2017. Reconstruction of the cranial musculature of the paraceratheriid rhinocerotoid Pappaceras meiomenus and inferences of its feeding and chewing habits. Acta Palaeontologica Polonica 62 (2): 259–271.

Wang, J.W. 1976. A new genus of Forstercooperinae from the late Eocene of Tongbo, Henan. Vertebrata PalAsiatica 14 (2): 104–111.

Wang, Y.Q. et al. 2010. Early Paleogene stratigraphic sequences, mammalian evolution and its response to environmental changes in Erlian Basin, Inner Mongolia, China. Science China: Earth Sciences 53 (12): 1918–1926.

Wang, Y.Q., J. Meng, and X. Jin. 2012. Comments on Paleongene localities and stratigraphy in the Erlian Basin, Nei Mongol, China. Vertebrata PalAsiatica 50 (3): 181–203.

Wood, H.E. 1934. Revision of the Hyrachyidae. Bulletin of the American Museum of Natural History 67 (5): 181–295.

Wood, H.E. 1938. *Cooperia totadentata,* a remarkable rhinoceros from the Eocene of Mongolia. American Museum Novitates 1012: 1–20.

Wood, H.E. 1963. A primitive rhinoceros from the late Eocene of Mongolia. American Museum Novitates 2146: 1–11.

Ye, J. 1983. Mammalian fauna from the late Eocene of Ulan Shireh area, Inner Mongolia. Vertebrata PalAsiatica 21 (2): 109–118.

Zhai, R.J. 1977. Supplementary remarks on the age of Changxindian Formation. Vertebrata PalAsiatica 15 (3): 173–177.

APPENDIX

Study Specimens and Measurements

1. Taxonomic Revision for Specimens Formerly Assigned to Forstercooperiinae

Species	Specimen number	Specimen	P1/p1	Revised taxonomy
F. totadentata	AMNH 20116 (type)	Fragmentary cranium with I2–P4	P1 present	*F. totadentata*
"F. shiwopuensis"	PGMV 714	Maxilla with P4–M2	?	*F. totadentata*
F. mazhuangensis	IVPP V5072 (type)	Fragmentary cranium with P1–M3	P1 present	*F. mazhuangensis*
F. mazhuangensis	IVPP V5072 (type)	Mandibles with p3–m3	P1 present	*F. mazhuangensis*
P. confluens	AMNH 26660 (type)	Cranium with complete dentition	P1 present	*P. confluens*
P. confluens	AMNH 26660 (type)	Mandibles with complete dentition	p1 present	*P. confluens*
P. confluens	AMNH 26666	Mandible with p3–m3	?	*P. confluens*
P. confluens	AMNH 26667	Isolated P2	?	*P. confluens*
"F. huhebulakensis"	IVPP V5770	Fragmentary cranium with P4–M3, mandible with p3–m3	?	*P. confluens*
P. meiomenus	IVPP V20254 (type)	Cranium with complete dentition	P1 absent	*P. meiomenus*
"F. minuta"	AMNH 26672 (type)	Fragmentary maxilla with C, M1–M3	P1 present	*P. minuta*
"F. minuta"	AMNH 26672(type)	Fragmentary mandible with p2–m3	p1 present	*P. minuta*
"F. minuta"	AMNH 26056	Mandibles with c, p1–m3	p1 present	*P. minuta*
"F. minuta"	AMNH 26643	Fragmentary cranium with C, M1–M3	P1 present	*P. minuta*
"F. minuta"	AMNH 26668	Fragmentary mandible with p1–m3	p1 present	*P. minuta*
"F. minuta"	AMNH 26669	Fragmentary juvenile mandible with deciduous p3–m2	?	*Pappaceras* sp.
"F. minuta"	AMNH 26670	Fragmentary cranium with P2–m1	P1 present	*P. minuta*
"F. minuta"	AMNH 26671	Fragmentary cranium with M3	?	*Pappaceras* sp.
"F. minuta"	AMNH 26677	Fragmentary mandible with p3–m3	p1 absent	*P. meiomenus*
"F. minuta"	AMNH 107848	Fragmentary juvenile mandible with deciduous p3–p4	?	*Pappaceras* sp.
"F. minuta"	AMNH 107849	Isolated M3	?	*Pappaceras* sp.

Species	Specimen number	Specimen	P1/p1	Revised taxonomy
"*F. minuta*"	AMNH 107851	Fragmentary mandible with i2, c and p2–p3	p1 absent	*P. meiomenus*
"*F. minuta*"	AMNH 107852	Fragmentary mandible with c and p2–m3	p1 absent	*P. meiomenus*
"*F. minuta*"	AMNH 107856	Mandibles with nearly complete dentition	p1 absent	*P. meiomenus*
"*F. minuta*"	AMNH F:AM 99662	Fragmentary juvenile mandible with deciduous p2–p3	?	Excluded from forstercooperiines
"*Forstercooperia* sp."	PGM V799, V806 and V807	Isolated M3, fragmentary mandibles with m1–m3	?	*Pappaceras* sp.
"*Forstercooperia* sp."	IVPP V5108, V5108.1 and V5109	Isolated p3 and p4, fragmentary mandible with m1–2	?	Excluded from forstercooperiines
"*Forstercooperia* sp."	IVPP V5241	Isolated P2, P4 and fragmentary maxilla with M1–M3	?	Excluded from f orstercooperiines
Pappaceras sp.	IVPP V5075	Fragmentary cranium with P1–M3	P1 present	*Pappaceras sp.*

2. Measurements of Upper Cheek Teeth of Specimens Assigned to Forstercooperiines (mm)

		F. totadentata		*F. ulanshirehensis*		*F. mazhuangensis*	*P. confluens*	*P. minuta*	*P. meiomenus*	*P.* sp.	
		AMHN 20116	PGM V714	AMNH 20168	IVPP V20154	IVPP V5072	AMHN 26660	AMHN 26672	IVPP V20254	IVPP V5075	PGM V799
	L	24.2		17.6		20.5	17.9		11.8	25.4	
P1	W	20.5		11.9		16.7	11.2		9.78		
	L	22.9		18.0		22.9	15.9		12.5	22.3	
P2	W	29.8		17.3		32.5	21.3		12.7	27.5	
	L	26.3		24.6	21.3[a]	28.8	17.1		13.8	33.4	
P3	W	38.5		25.8	29.2[a]	37.0	26.4		18.2	37	
	L	31.0		25.4	26.8	29.9	19.7		15.6	26.8	
P4	W	45.4	38[a]	31.3	34.4[a]	42.7	29.1		23.4	41	
	L		44	36.5	38.5	37.4	24.8	22.4	24.3	34.5	
M1	W		51	35.9	34.8	40.2	30.1	23.3	26.4		
	L		51	39.9	47	47.5	31.4	26.8	30.2	39.4	
M2	W		52.8	43.3	42.6	47.5	31.9	27.6	27.4	43.3	
	L			33.2	41.1[a]	42.0	31.9	26.0	28.5	37.9	35.0
M3	W			41.0		45.8	35.2	27.0	28.2	41.5	40.5
P1–P4	L	108.5		81.4		103.2	71.1				
M1–M3	L			106.7	123.0	118.0	87.1	78.6[a]	80.9	108.5	

[a] Approximate measurements.

3. Measurements of Lower Cheek Teeth of Specimens Assigned to Forstercooperiines (mm)

		F. ulanshirehensis			*F. mazhuangensis*	*P. confluens*			*P. minuta*			*P. meiomenus*				*P.* sp.
		IVPP V20155	IVPP V20156	AMNH 22101	IVPP V5072	AMHN 26660	AMNH 26666	IVPP V5771	AMHN 26672	AMNH 26056	AMNH 26668	AMNH 26677	AMNH 107851	AMNH 107852	AMNH 107856	AMNH 26669
	L	19.0	17.2			13.9				10.8	11.2					
p1	W	10.4	11.0			8.3				5.40	7.8					
	L	18.6	19.6			16.1			12.3	14.6	12.6		13.4	10.9		
p2	W	11.0	13.6			9.9			7.5	8.4	9.2		8.6	7.5		
	L	25.2	21.5[a]	23.3[a]	28.9	19.6	18.1	13.7	15.1	19.1	16.4	14.3	15.4	13.3	13.2	18.7
p3	W	14.5	16.8[a]	15.4[a]		12.8	11.3	10.2	8.5	11.0	12.0	8.8	10.1	9.4	9.52	10.1
	L	29.0	27.3	29.4	23.3	21.1	19.7	16.0	17.6	17.2	17.6	16.2		14.8	15.5	17.9
p4	W	17.2	20.0	17.4		14.0	13.9	12.9	11.6	13.3	13.4	11.8		11.4	11.2	11.5
	L	35.3		31.0	34.0	25.0	26.4	22.2	24.0	23.2	22.3	23.2[a]		19.2	19.3	19.9
m1	W	22.6		22.2	23.6	18.0	17.9	17.0	14.2	17.5	16.4	16.4[a]		14.6	14.9	13.4
	L	43.3		37.4	40.9	30.8	27.2	26.3	26.0	25.0	25.3	25.6		24.1	24.8	24.3
m2	W	26.0		25.4	27.4	19.2	19.4	17.7[a]	15.5	17.7	18.8	*15.2[a]		15.9	16.6	14.3
	L	46.1		37.9	44.0	35.5	28.7		26.7[a]	27.2	28.3	26.3		26.3	28.7	
m3	W	27.5		24.8	28.0	19.7	18.8	17.0[a]	14.5[a]	18.3	17.1	15.5		15.6	16.3	
p1–p4	L	92.8	85.0			71.8				*61.6[a]	57.5					
m1–m3	L	129.5		110.5		89.1	82.9		75.9[a]	76.6	75.3	75.7[a]		69.05	70.8	

[a] Approximate measurements.

All issues of *Novitates* and *Bulletin* are available on the web (http://digitallibrary.amnh.org/dspace). Order printed copies on the web from:
http://shop.amnh.org/a701/shop-by-category/books/scientific-publications.html

or via standard mail from:

American Museum of Natural History—Scientific Publications
Central Park West at 79th Street
New York, NY 10024

♾ This paper meets the requirements of ANSI/NISO Z39.48-1992 (permanence of paper).